激光与光电子学进展 先进成像

共聚焦激光扫描检眼镜研究进展与应用(特邀)

叶夏笛[1,2],黄江杰[1,2],孔文[1,2],邢利娜[1],何益[1,2*],史国华[1,2]

[1]中国科学院苏州生物医学工程技术研究所江苏省医用光学重点实验室,江苏 苏州 215163;

[2]中国科学技术大学生物医学工程学院(苏州),生命科学与医学部,江苏 苏州 215163

摘要 眼底成像对眼科学研究、眼底疾病诊断和治疗都有着重要的意义,而共聚焦激光扫描检眼镜由于具有优越的成像质量和泛用性,并具有独特的轴向分辨能力,在眼底成像领域中已经占据主导地位。主要综述了共聚焦激光扫描检眼镜检查法在超广角眼底成像方面和高分辨率眼底成像方面的实现原理和技术发展,分析了目前仍面临的挑战,并基于现存的挑战对其未来发展进行展望。

关键词 眼科光学与器件;超广角眼底成像;高分辨率眼底成像;共聚焦激光扫描检眼镜

中图分类号 TH786 **文献标志码** A **DOI**: 10.3788/LOP240437

Research Progress and Application of Confocal Scanning Laser Ophthalmoscope (Invited)

Ye Xiadi[1,2], Huang Jiangjie[1,2], Kong Wen[1,2], Xing Lina[1], He Yi[1,2*], Shi Guohua[1,2]

[1]*Jiangsu Key Laboratory of Medical Optics, Suzhou Institute of Biomedical Engineering and Technology, Chinese Academy of Sciences, Suzhou* 215163, *Jiangsu China*;

[2]*Division of Life Sciences and Medicine, School of Biomedical Engineering (Suzhou), University of Science and Technology of China, Suzhou* 215163, *Jiangsu China*

Abstract Fundus imaging plays a vital role in research on the ophthalmology, diagnosis, and treatment of fundus diseases. Confocal scanning laser ophthalmoscope has superior imaging quality, wide applicability, and unique axial resolution, making it dominant in fundus imaging. We present a review of the principle and technical developments of confocal scanning laser ophthalmoscopy in ultra-widefield and high-resolution fundus imaging and analyze the challenges of confocal scanning laser ophthalmoscopy. Finally, we discuss the future development prospects based on existing challenges.

Key words ophthalmic optics and devices; ultra-widefield fundus imaging; high-resolution fundus imaging; confocal scanning laser ophthalmoscope

1 引 言

眼睛是人类获取外界信息最重要的器官,在人类所获取的信息量中有80%以上是通过视觉获得的。眼底是眼球后部的多层组织结构,其中视网膜是眼底最重要的一层膜状组织,当光信号投射在视网膜上时,视网膜会产生光化学反应将光信号转化为神经生物电信号,再经视网膜底部的神经元传递到大脑神经中枢,从而产生视觉感知[1]。然而,眼底疾病会对眼底的正常生理结构和功能产生影响,例如:中心性浆液性脉络膜视网膜病变[2]、视网膜静脉阻塞[3]、糖尿病性视网膜病变[4]、年龄相关性黄斑病变[5]等。这些疾病在早期症状中并不明显,难以及时地发现并控制,待出现明显的症状时患者的视力就已经受到了不可逆转的损伤,严重者还会完全丢失视力,对患者的生活质量产生了极大的影响,因此,眼底疾病的早期检查对疾病的预防和治疗至关重要。

对眼底结构的直接观测是评估眼底疾病行之有效的手段,随着科学技术的发展,借由光学手段观察人眼

收稿日期:2024-01-03;**修回日期**:2024-01-23;**录用日期**:2024-01-24;**网络首发日期**:2024-02-20

基金项目:国家自然科学基金(62075235)、国家重点研发计划(2021YFF0700700)、中国科学院青年创新促进会(019320)、中国科学院战略性先导科技专项(XDA16021304)

通信作者:*heyi@sibet.ac.cn

眼底成为了可能。早在19世纪就已经出现了用于观察眼底的检眼镜。20世纪50年代，德国蔡司通过引入感光元件和电子闪光技术，成功设计出第一台可以数字化记录眼底图像的眼底相机[6]，也称泛光照明检眼镜（Flood illumination ophthalmoscope，FIO），并广泛用于临床检查。1980年，Webb等[7]提出了激光扫描检眼镜（Scanning laser ophthalmoscope，SLO），该检眼镜因为提高了光能利用率和使用了更灵敏的光探测器，使入射到眼底的光功率随之降低，所以患者的舒适性和安全性得以提高。后来该作者又进一步将共聚焦原理与SLO系统结合提出了共聚焦激光扫描检眼镜（Confocal scanning laser ophthalmoscope，CSLO）[8]，不但消除了离焦背景光，眼底图像的信噪比和对比度显著提高，而且还具备了光学层析的能力。经过了三十多年的改进，CSLO在临床眼底成像方面已经占据了明显的优势地位。

早期的检眼镜只能提供30°～50°的视场，导致其在临床应用中因无法观测到位于视网膜周边的病理部位而容易出现漏诊，从而延误了对病情的治疗。因此，扩大眼底成像范围一直是检眼镜发展的目标之一，随着眼底成像范围被逐渐扩大，广角、超广角的概念相继出现，发展至今，最大的眼底成像范围已经超过了200°，涵盖了眼底的绝大部分区域，对诊断及评估眼底疾病发挥了重要作用。

随着眼底成像范围的扩大，提高眼底成像分辨率的需求也被提出。眼底疾病在早期引起的单细胞或亚细胞结构变化的可视化有助于疾病诊断并对患者予以及时的治疗，阻止病情进一步恶化，还能深入地研究眼底疾病的病程发展，因此，眼底的高分辨成像对眼底疾病的早期检查和科学研究具有重要意义。检眼镜以人眼作为物镜，以视网膜作为成像物，人眼的瞳孔直径为1～8 mm，对应的数值孔径为0.03～0.23，在常用的照明光波段下，理论上横向分辨率极限约为2 μm[9]。然而，传统检眼镜的横向分辨率受到了人眼光学像差的限制。自适应光学（Adaptive optics，AO）技术的引入不仅校正了人眼光学像差，显著提高了人眼的光学质量，还使高分辨率眼底成像成为可能。

本文介绍了CSLO在超广角眼底成像方面和高分辨率眼底成像方面的发展与应用。从眼底成像视场的定义开始，分别介绍了接触式超广角CSLO和非接触式超广角CSLO，然后总结了目前商用的超广角CSLO。在引入人眼的波前像差对眼底图像分辨率的影响之后，介绍了AO技术与检眼镜结合的实现原理及几个主要科研机构的技术改进，紧接着归纳总结了高分辨率眼底成像技术的典型应用，最后分析了CSLO目前仍面临的挑战，并基于现存的挑战对其未来发展进行展望。

2 超广角眼底成像技术

2.1 眼底成像视场的定义

德国卡尔·蔡司集团生产的第一台商用泛光照明检眼镜视场为20°，一段时间后被提升到了30°，在临床上得到了广泛应用[6]。因此，在早期，临床上一般称30°及以内的视场为正常视场，大于30°的为广角视场。然而，随着临床诊断需求的增长，眼底成像的正常视场被进一步扩大到30°～50°，超广角的概念也随之出现，但业内对于广角视场和超广角视场的界限一直没有统一的划定。2019年，国际眼科专家在会议上对眼底成像视场范围的定义给出了建议[10]，定义后极部视网膜血管拱之内的视场为正常视场，视网膜血管拱到漩涡静脉壶腹部后缘之间的视场为广角视场，以中心凹为中心在四个象限中都能看到漩涡静脉壶腹部前缘的视场为超广角视场，能一次性看清整个视网膜的视场为全视场，角度范围定义见表1，示意图见图1。

表1 眼底成像视场定义[10]

Table 1 Definition of field of view of fundus imaging[10]

Region	Field of view	Anatomic location
Normal field of view	0°–50°(normal field)	Within retinal vascular arcades
Wide angular field	60°–100°(wide field)	Edge of retinal vascular arcades to posterior edge of vortex vein ampulla
Ultra wide angular field	110°–220°(ultra-wide field)	Anterior edge of vortex vein ampulla and beyond to pars plana
Full field of view	360°(whole field)	Entire retina

2.2 接触式超广角共聚焦激光扫描检眼镜

在SLO被提出之前，对视网膜周边进行成像只能借助于FIO。1971年，Pomerantzeff等[11]基于FIO提出了一种接触式广角检眼镜的设计方案，使用光纤连接角膜接触镜经过瞳孔照明和巩膜透照扩大眼底的照明范围，并于1975年将其付诸现实，实现了148°的眼底成像视场[12]。采用类似于Pomerantzeff的方法，基于FIO的商用超广角眼底成像设备Retcam[13]、Panoret-1000[14]等相继出现。

在SLO被提出后不久，使用角膜接触镜扩大SLO成像视场的可行性得到了验证[15]。2005年，Staurenghi等[16]设计了一种集成式大视场透镜系统，如图2所示，其包含两个双凸非球面透镜和一个二元凹凸角膜接触镜，并与CSLO结合，使眼底成像视场扩大5倍，达到了150°，并成功应用于眼底荧光造影成像。

无论是基于FIO还是基于CSLO的接触式检眼镜，它们都有着两个共同的缺点。一是需要使用角膜接触镜直接接触人眼，这会对患者造成极大的不适；二

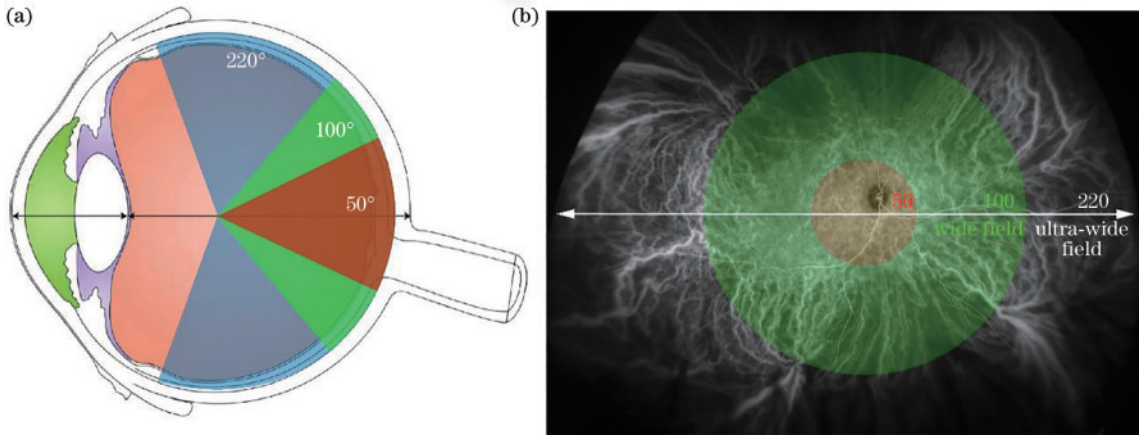

图 1　眼底成像视场范围示意图。(a)人体解剖学中眼球侧面解剖图;(b)眼底成像仪器 Optos 采集的吲哚菁绿造影图,图中可以看见四个涡旋静脉

Fig. 1　Schematic diagram of field of view range for fundus imaging. (a) Lateral image of human eye from e-anatomy; (b) indocyanine green angiography image collected with Optos, in which four vortex veins can be seen

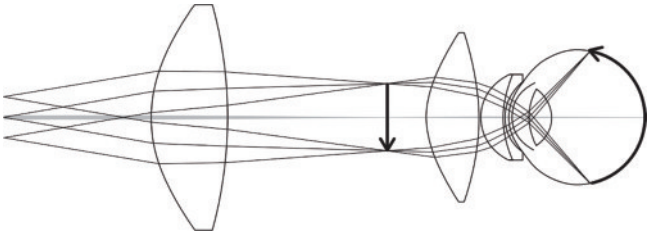

图 2　用于超广角眼底成像的集成式角膜接触镜[16]

Fig. 2　Integrated corneal contact lens for ultra-widefield fundus imaging[16]

是需要一位熟练的操作人员在成像时保持设备对准角膜接触镜,且采集流程繁琐,对操作人员的要求比较高。

2.3　非接触式超广角共聚焦激光扫描检眼镜

在接触式超广角检眼镜快速发展的同时,随着非球面镜片加工技术的进步,通过非接触式成像的方法实现眼底的广角甚至超广角成像成为可能[17-20]。由于具有患者舒适度高、操作简单等优点,非接触式超广角检眼镜逐渐成为主流,直至今天,比较常见的商用非接触式超广角检眼镜有德国蔡司集团的 Clarus、日本尼德克集团的 Mirante、德国海德堡医疗集团的 Spectralis、英国欧堡医疗集团的 Optos 和中国微清医疗集团的 CRO-PLUS 等。各类商用非接触式超广角 CLSO 的参数如表 2 所示。

当成像视场较小时,可以将眼底近似为等晕平面进行光学设计,但是随着成像视场的扩大,眼底不能再被近似为平面,需要对光学系统重新进行设计,才能确保成像时视网膜与探测器共轭,实现眼底大视场清晰成像。以微清医疗集团 CRO-PLUS 为代表的超广角 CSLO,针对性地设计光学系统,缩短工作距离从而增大光束扫描角度,以达到扩大成像视场的目的。CRO-PLUS 成像时无需散瞳,在 1.5 mm 瞳孔直径下即可实现最大单张 160°视场的眼底成像,通过图像拼接技术还可将成像视场进一步扩大至 240°,且仅通过软件一键操作便可切换不同的成像视场,与海德堡 Spectralis 系统通过更换成像镜头来实现不同视场成像的方法相比,微清医疗集团的 CRO-PLUS 在操作上显得更为简单快捷。

英国欧堡医疗集团的 Optos 是目前世界上单次成像视场最大的超广角检眼镜。Optos 超广角原理如图 3 所示,其原理利用了椭球的光学性质,当光线经过椭球其中一个焦点并被椭球反射后,必定会经过椭球的另外一个焦点。将 CSLO 和椭球镜相结合,把人眼瞳孔固定在椭球镜的一个焦点 F_2 处,当激光从另一个焦点 F_1 射向椭球镜时,经过椭球镜反射后便会经过瞳孔进入眼睛[21]。这种设计扩大了 CSLO 的扫描角度,在无散瞳的情况下能够实现单次成像 200°的眼底视场。在患者配合和散瞳的情况下,通过眼位引导和图像自动拼接技术,可以使眼底成像视场扩大到 220°。发展至今,多模态 Optos 系统已经配备了多个激光波段,能够实现眼底的伪彩色成像、眼底自发荧光(Fundus autofluorescence, FAF)成像,以及荧光素钠造影(Fluorescein angiography, FA)成像、吲哚菁绿造影(Indocyanine green angiography, ICGA)成像等。此外,CSLO 和椭球镜的结合具有非常大的焦深,使其能够对深层的葡萄膜瘤成像[22]。

Optos 的优势同样造就了它的缺点。首先,视网膜是一个三维立体球面,在成像时将其转换为二维平面图像会造成周边出现不同程度的失真[23-24];其次,整个范围内眼底图像的对比度不均匀,特别是在无散瞳的情况下[24];然后,大焦深会造成睫毛或者眼睑伪影[25];最后,同时使用多个激光波段会造成伪色[26],无法提供真实的彩色图像。为了克服这些缺点,Optos 通过在成像软件中采用一种立体投影算法校正了图像周边的失真,并增强了视网膜图像后极部和周边的对比度,使其更加均匀,同时还减少了伪影[27-28]。

表 2 商用非接触式超广角 CSLO

Table 2 Commercial non-contact ultra-widefield CSLO

Product	Maximum field of view /(°)	Imaging mode	Device photo	Display of imaging effect
Clarus	133	Color, red, green, blue, FAF, IR		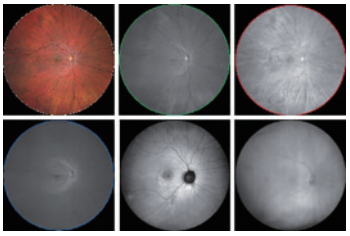
Mirante	163	Color, FA, FAF, ICGA, retro		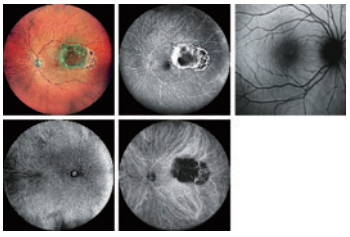
Spectralis	102	FA, ICGA, IR, FAF		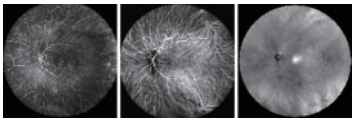
Optos	200	Pseudo color, RF, FAF, FA, ICGA, choroid		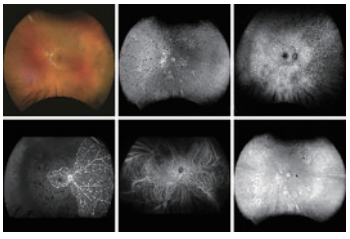
CRO-PLUS	160	Color, RF, FAF, FA, ICGA, IR		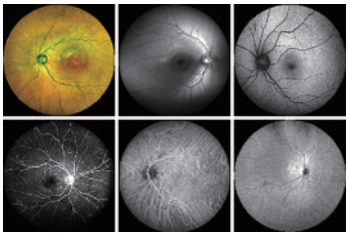

Note RF: red free; IR: infrared ray. Order of imaging effect images arranged from left to right corresponds one-to-one with order of imaging modes. All images are referenced from respective product online pages.

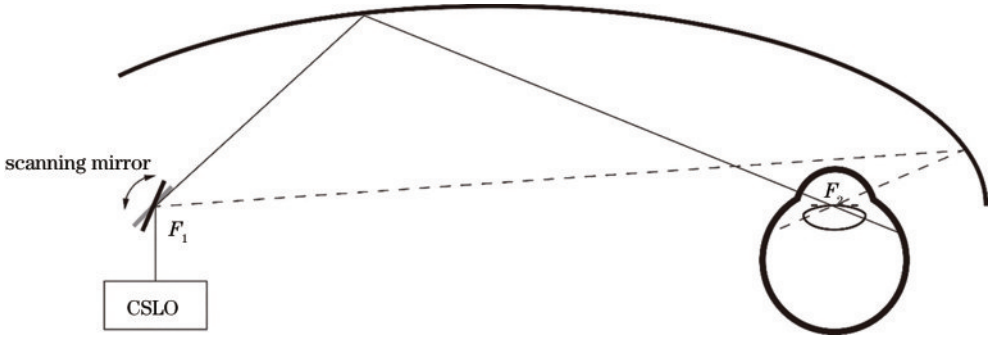

图 3 Optos 超广角 CSLO 原理

Fig. 3 Principle of Optos ultra-widefield CSLO

值得注意的是，CSLO的成像方式是用激光点对整个视场进行光栅扫描成像，其成像速率受扫描速度和探测器曝光时间的综合影响，而在固定瞳孔大小下的横向分辨率则受扫描分辨率的影响[8]。在不牺牲眼底图像质量的情况下，随着眼底成像视场的扩大，需要扫描的成像点也随之增多，换言之，眼底成像的帧率也会随之降低。因此，现有的商用超广角CSLO一般只能单帧成像或是低帧率（<10 frame/s）成像[29]。有研究表明，将CSLO的点扫描模式替换为线扫描模式可以显著提升帧率[30-33]。如图4所示，在线扫描CSLO中，激光光源经过柱面透镜时会生成一条细长的激光线，先使用共聚焦狭缝代替共聚焦针孔，然后对眼底进行一维扫描成像，与原本的激光点二维扫描成像相比，仅略微牺牲了沿激光线方向上的分辨率便能使成像帧率大大提高，还简化了系统的光路结构。除此以外，增加扫描光束数量[34]、使用更快速的扫描装置[35]配合响应速度更快的探测器也能在一定程度上提升帧率。

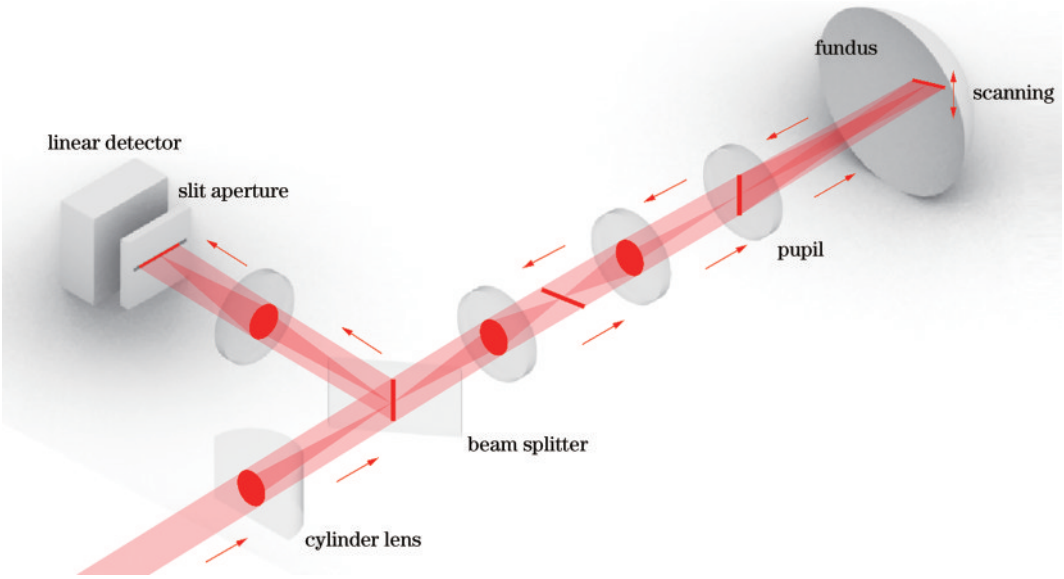

图4　线扫描光路（图中未画出扫描装置）

Fig. 4　Line scanning light path (scanning device is not shown)

3　高分辨率眼底成像技术

随着CSLO的成像视场越来越大，能被可视化检查的眼底病变图像也逐渐完整，为了进一步研究眼底疾病的起因和发展过程，加深对其的理解，人们在扩大眼底检查范围的同时，对精细分辨病灶的需求也越来越高。然而，人眼不是一个完美的光学系统，人眼的波前像差将CSLO的横向分辨率限制在了10～15 μm，远没有达到理论衍射极限分辨率2 μm。将AO技术引入CSLO，就是为了测量和校正人眼的波前像差，以提高眼底图像的分辨率和图像质量。

3.1　人眼的波前像差

人眼的波前像差是指光通过实际人眼产生的波面和理想人眼产生的波面之间存在的偏差，包含色差和单色像差，在理想的人眼中，眼底上一个点发出的理想球面波前从人眼出射后应为理想平坦波前，而正常人眼存在的像差会导致出射波前为畸变波前，如图5所示。色差是因为不同波长的光在人眼介质中的折射率不同，导致不同波长的光落在视网膜上的位置不一样，所以色差可以用单色光源来克服。单色像差与波长无关，影响单色像差的因素有很多，包括泪膜、角膜和晶状体各自的形状不规则特性，以及每个部分之间的离轴和相对倾斜，通常分为低阶像差和高阶像差。离焦和散光等低阶像差所占比例最大（>90%），可以使用球面透镜和柱面透镜来校正。虽然高阶像差所占比例相对较小（<10%），但却难以通过光学设计的方法来校正，而且研究表明，随着瞳孔的增大，高阶像差会显著降低人眼的横向分辨率和眼底图像质量[36]，而在眼底检查中，往往会为了提高衍射极限分辨率而对人眼进行散瞳处理，因此高阶像差对成像分辨率的影响不容忽视[37]。

为了使人眼波前像差的测量具有可比性和可重复性，一般会选取人眼的入瞳作为测量的参考位置。常用Zernike圆多项式的线性组合对波前像差进行描述，其优势在于Zernike圆多项式的低阶项和Sidel像差相对应，且可以让不同级的像差彼此平衡并使高斯焦点的强度达到最大，即让像差的校正效果达到最佳[39]。

3.2　人眼波前像差的校正

1997年，Liang、Williams和Miller[40]将AO技术引入到检眼镜中，提出了自适应光学泛光照明检眼镜（Adaptive optics flood illumination ophthalmoscopy，AOFIO），率先将AO技术用于测量并校正人眼像差，获得了活体视网膜单细胞级高分辨率图像。2002年，Roorda等[41]进一步将AO技术与CSLO结合，研制了

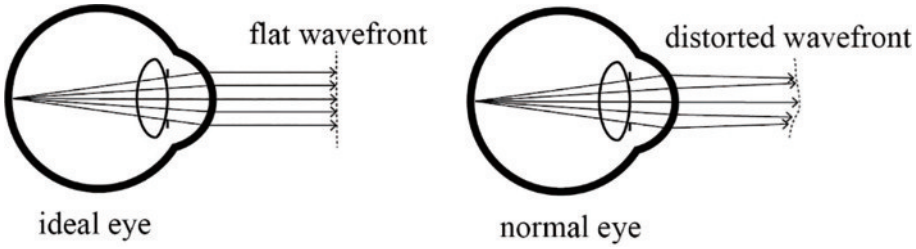

图 5　理想人眼和正常人眼的波前形状[38]

Fig. 5　Wavefront shapes of ideal eye and normal eye[38]

自适应光学扫描激光检眼镜(Adaptive optics scanning laser ophthalmoscopy, AOSLO),其光学成像质量要优于AOFIO。在国内,中国科学院光电技术研究所最早开始了AO技术与检眼镜结合的相关研究,并取得了一系列的研究成果[42-45]。2009年,中国科学院光电技术研究所成功研制了国内第一台AOSLO临床样机,获得了高分辨率的眼底图像,并在其后开展了超分辨视网膜成像的相关研究,进一步提高了AOSLO的分辨率[46-47]。

基于硬件实现波传感和波前校正的AO系统常用在高分辨率眼底成像中,该系统通常包含三个部分:波前传感器、波前校正器和波前控制器。如图6所示,AO系统的基本工作流程:先用参考平行光束照射波前传感器确定参考基准,再用一束激光入射到眼底形成一个光点作为信标导星,眼底反射回来的信标光束携带着人眼像差的信息进入波前传感器完成对人眼像差的测量,然后传递给波前控制器,经过波前控制器解算复原得到需要校正波前的电压信号,再传递给波前校正器,实现对人眼像差的闭环校正,像差校正后的成像光束再被探测器接收从而实现高分辨率的眼底成像。波前校正的效果是双向的,一是确保在眼底形成聚焦良好的信标导星,二是确保在探测器处形成聚焦良好的成像点。

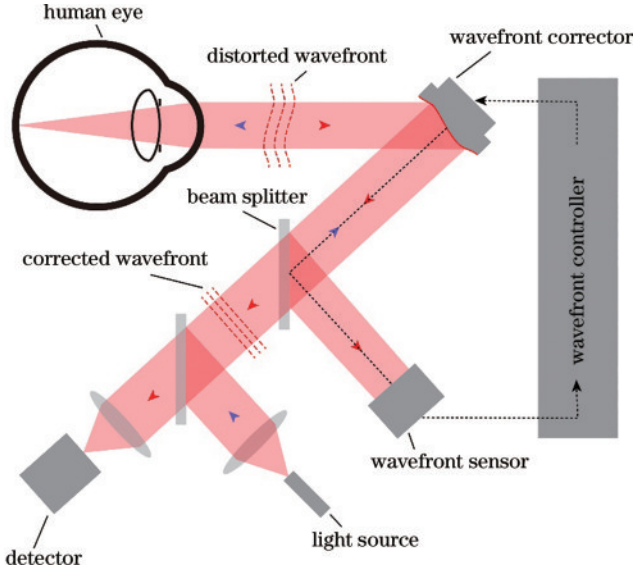

图 6　通用眼底成像AO系统

Fig. 6　General fundus imaging AO system

波前像差实质上是相位的变化,因此测量并改变畸变波前不同处的相位,就能达到波前校正的目的。在人眼眼底成像中,应用最为广泛的波前传感器为Shack-Hartmann波前传感器(Shack-Hartmann wavefront sensor, SHWS),它能够直接测量出波前的斜率从而确定波前的相位。常与SHWS配合使用的波前校正器为可变形镜(Deformable mirror, DM),它可以通过改变镜面形状来直接调控波前相位,除此以外,液晶空间光调制器和分段镜也能作为波前校正器使用[48]。而连接SHWS和DM的波前控制器一般为通用计算机,主要作用为利用波前复原算法[49]将SHWS测量到的波前斜率转换为DM校正波前的控制信号,形成像差校正的闭环。AO技术与检眼镜的结合,突破了人眼波前像差的障碍,使横向分辨率达到了衍射极限分辨率,人眼眼底各类精细结构的活体可视化得以逐渐实现。

3.3　自适应光学扫描激光检眼镜

2002年,Roorda等[41]将AO与CSLO结合形成了AOSLO,在实时校正人眼像差的情况下,实现了视网膜衍射极限高分辨率成像。AOSLO光路结构如图7所示,光源发出的光经过准直后进入传输光路,经DM、水平扫描仪(HS)、垂直扫描仪(VS)等器件反射,最后到达眼底。眼底反射的光大部分按原路返回,小部分光透过翻转镜(FM)到达SHWS,SHWS与计算机(PC)相连,用于测量人眼波前信息,PC根据探测到的波前信息产生控制信号,通过闭环控制DM完成像差校正。在完成像差校正的前提下,大部分眼底反射光经FM反射进入PMT,通过与双轴扫描HS、VS同步,重构获取没有像差影响的视网膜衍射极限高分辨率图像。在图7中,L为透镜,M为反射镜,FO为光纤光源,AP为人工瞳孔,BS为分束镜,LA为微透镜阵列,CP为共焦小孔,PMT为光电倍增管,r点为视网膜,p点为瞳孔共轭处,HS扫描频率为16 kHz,VS扫描频率为30 Hz。

该AOSLO系统在7 mm的瞳孔直径下,眼底成像的横向分辨率大约为2.5 μm,纵向分辨率大约为70 μm,帧率达到了30 frame/s[41]。成像结果如图8所示,其中左图和右图分别为对视网膜相同区域AO像差

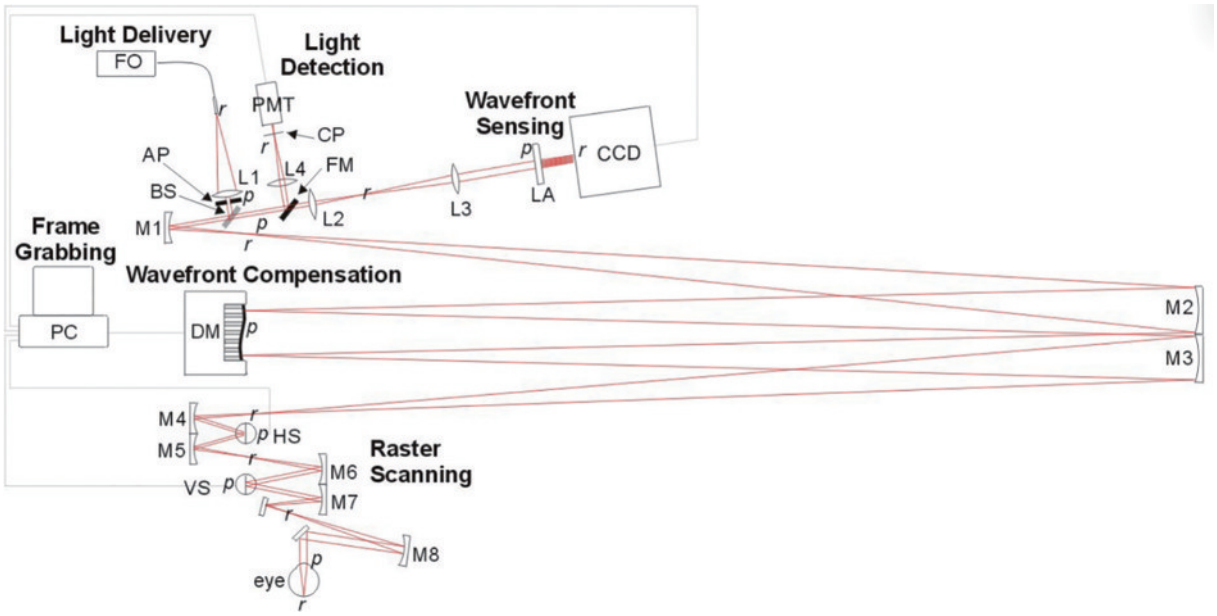

图 7　AOSLO 光路结构示意图[41]

Fig. 7　AOSLO optical path structure diagram[41]

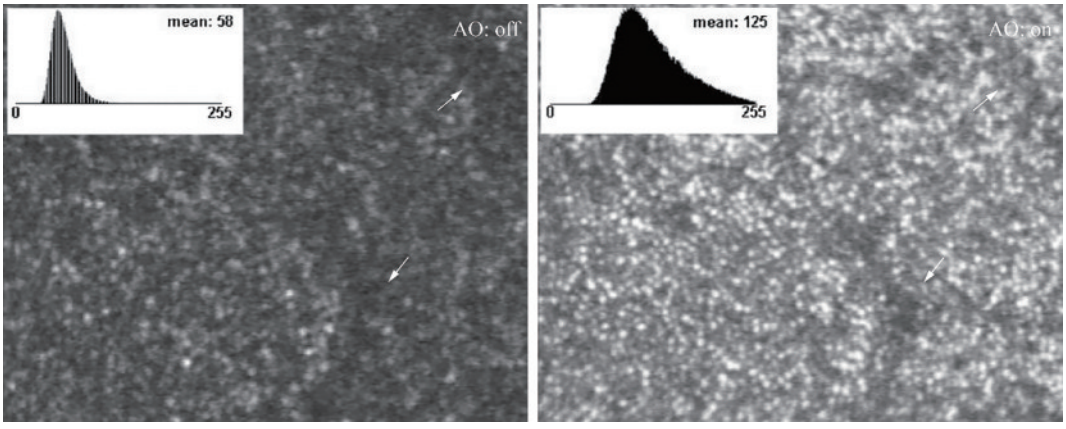

图 8　AOSLO 成像结果[41]

Fig. 8　AOSLO imaging result[41]

校正和 AO 校正前后的成像结果，箭头所指处的阴影为视网膜毛细血管，插图为图像的灰度直方图。相较于关闭 AO 校正，开启 AO 校正后得到的图像整体灰度值和对比度都得到了提高，光感受器和视网膜毛细血管可以被清晰分辨。在 Roorda 等研制出第一台 AOSLO 之后，有多个课题组跟进了他们的研究并进行改进，使得 AOSLO 的分辨率、视场及成像速度等性能指标得到了进一步提高，并极大地扩展了其功能和应用。相关科研机构的 AOSLO 的技术改进及成果如表 3 所示。

在 AOSLO 的众多性能指标中，视场是其中极为重要的一个指标。受人眼像差非等晕性的影响，AOSLO 的成像视场一般都被限制在 1°～2°之间，导致诸如无法重复成像、成像位置不明确等问题。为了扩大高分辨率眼底成像的视场，目前已经提出了 3 种方法来解决该问题，但它们都存在一定的局限性，具体总结如表 4 所示。

4　AOSLO 在视网膜成像中的应用

4.1　视网膜结构性成像

4.1.1　光感受器细胞

光感受器细胞作为视觉的起点，包括视锥细胞和视杆细胞两类，是视网膜中最先被研究的结构，直到今天，光感受器仍然是眼科研究中的主要焦点，这归因于以下两点：1）视锥细胞具有波导特性[89]，在内外节段的交界处和锥体外节段的尖端处有非常强的反射能力，这使得它们具有高内在对比度，是最容易成像的细胞[90]；2）光感受器细胞的结构、密度、反射率等因素跟眼底疾病之间的联系仍然有尚未解决的问题。多年来的技术进步使 AOSLO 的成像能力获得了显著提高，视锥细胞可分辨的成像区域逐渐向视网膜中央凹的中心靠近，同时尺寸接近衍射极限分辨率的视杆细胞也已被 AOSLO 分辨，如图 9 所示[56]。值得注意的是，

表 3 相关科研机构的 AOSLO 的技术改进及成果

Table 3 Technical improvement and achievement of AOSLO by major institute

Institute	Improvement	Achievement
University of Rochester (USA)	1) Replaced confocal pinhole with annular pupils[50]. 2) Developed split-detection mode[51] and dark field mode[52]. 3) Developed close-loop optical stabilization[53] and fast registration[54]. 4) Designed reflective afocal broadband AOSLO[55]	1) Improved resolution. 2) Imaged human cone photoreceptor inner segment and retinal pigment epithelium without label. 3) Solved problem of high-resolution retinal image blurring caused by nystagmus. 4) Reduced astigmatism of pupil and retinal conjugate surfaces simultaneously. 5) First obtained human rod cell image[56] and single neuron image in ganglion cell layer[57]
University of California, Berkeley (USA)	1) Designed compact AOSLO based on microelectromechanical DM[58]. 2) Developed synchronous laser modulation technology and retinal stability tracking technology[59-63]. 3) Developed motion contrast imaging technology[64]. 4) Designed scheme of versatile multi-detector[65] and multi-wavelength imaging[66], and further design wide convergence, multi-spectral AOSLO[67]	1) Reduced device volume. 2) Delivered a highly stable and aberration corrected stimulation to a single retinal cone cell, and simultaneously reduce influence of nystagmus so that expanded high-resolution imaging field. 3) Achieved non-invasive capillary imaging and flow velocity measurements without any contrast media[68]. 4) Expanded imaging channel, and achieve multi-channels aberration corrected simultaneously. 5) Studied effects of fixational tremor on retinal image[69-70]
University of Indiana (USA)	1) Combined wide field SLO with AOSLO and further integrate[71-73]. 2) Developed off-set aperture mode[74-75]. 3) Developed spatiotemporal scanning mode with vertical scanning stopped[76-77]. 4) Developed high speed polarimeter based on AOSLO[78-79]. 5) Developed dual-channel scanning mode[80]. 6) Replaced dot scanning mode with line scanning mode[81]	1) Reduced influence of nystagmus, and location of high-resolution imaging can be obtained, so it is possible to achieve repeated imaging of the same area. 2) Achieved fine structural imaging of vascular wall. 3) Achieved fast measurement of retinal blood flow. 4) Reduced calculation error of polarization caused by nystagmus, and use polarization characteristics to improve the contrast of retinal structure. 5) Improved frame rate without increasing system complexity. 6) Extremely reduced influence of nystagmus and improve frame rate. 7) Template free eye motion correction[82]
Chinese Academy of Sciences Institute of Optics and Electronics (China)	1) Replaced confocal pinhole with specially designed pupil filter[47]. 2) Introduced KLT-SIFT algorithm in image tracking[83-84] and develop image auto-montage technology based on algorithm[85]. 3) Designed bimorph DM based compact AOSLO[86-87]	1) Improved resolution. 2) Reduced image distortion caused by nystagmus and seam artifacts. 3) Improved correction stroke and accuracy. 4) First achieved measurement of blood oxygen saturation for small blood vessels below 50 μm[45]

表 4 扩大高分辨眼底成像视场的方法

Table 4 Method for increasing field of view of high-resolution fundus imaging

Method	Disadvantage	Field of view	Author/Product
Dual-conjugate adaptive optics	As field of view increase, complexity of system will definitely increase	4°×4°	Laslandes[88]
Reduce pupil diameter	Reducing pupil size will decrease lateral resolution	4°×4°	Imagine Eyes-rtx1 (AOFIO)
Correct aberrations in multiple fields separately	As field of view increase, imaging time also increase	3°×5°	Physic Science Inc-CAORI[81]

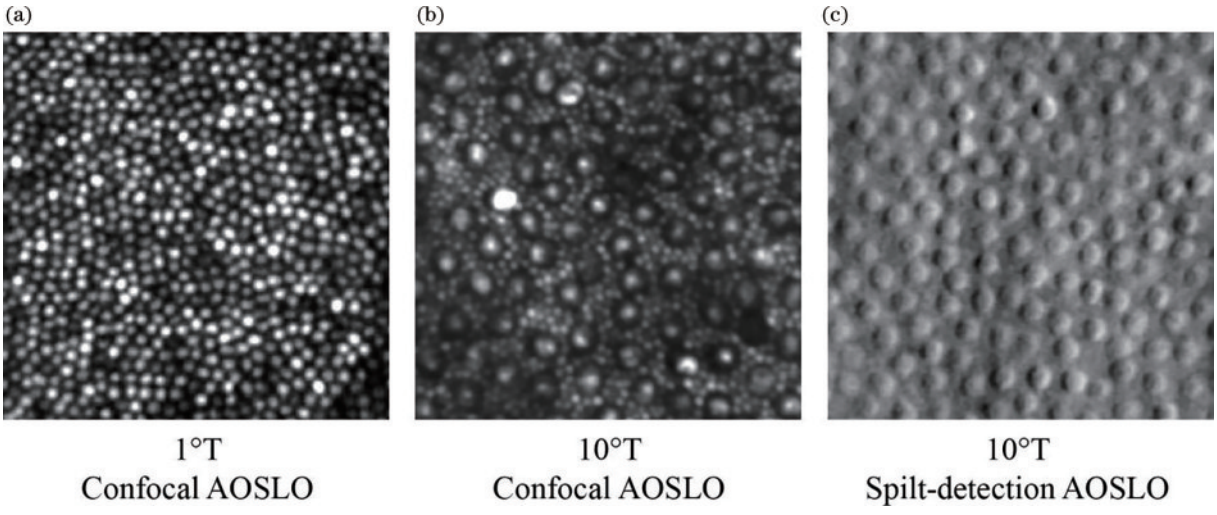

图 9　AOSLO 获取的人眼光感受器图。(a)中心凹颞侧 1°偏心处，图中亮点为视锥细胞[51]；(b)中心凹颞侧 10°偏心处，图中显示了完整的视锥细胞(大细胞)，间隙中镶嵌的亮点为视杆细胞[56]；(c) 中心凹颞侧 10°偏心处，图中显示的是视锥细胞的内节段，间隙中的视杆细胞内节段因尺寸太小而无法被分辨[51]

Fig. 9　Human eye photoreceptor image obtained from AOSLO. (a) At 1° eccentricity of temporal side of fovea, bright spot in image is cone cells[51]; (b) at 10° eccentricity of fovea shows intact cones (large cells) with rod cells embedded in space[56]; (c) at inner segment of cone cells is shown at 10° eccentricity of temporal side of fovea, image shows inner segment of cone cells, inner segment of rod cells in gap cannot be distinguished due to its small size[51]

AOSLO 的共焦图像并不能包含光感受器结构的全部信息，凭借单一的成像方式有可能会对视网膜的结构产生错误的认识，因此需要借助其他的方式进行补充理解。图 9(c)是分裂探测 AOSLO 所获得的视锥细胞内节段图像，其中分裂探测 AOSLO 依赖的是内节段的多重散射光，成像区域是外节段与内节段交界处的椭球区[51]。在正常的共焦图像和分裂探测图像中，每个视锥细胞和每个锥细胞内节段都有着一一对应的关系，当外部节段缺失或者其他因素导致视锥细胞不再反射后，在共焦图像的相应位置会表现为一个空洞，而分裂探测图像可以用来确定视锥细胞的内节段是否依然存在。光感受器的可视化使得定量分析其形态结构得以实现，通过识别和分割单个光感受器[91-92]，可以测得光感受器的密度、大小、间距和规则性等指标[93-95]。

4.1.2　血管系统

视网膜组织的代谢需求极其旺盛，分布在视网膜上丰富的血管网络能够满足其代谢需求，因此视网膜的健康和功能依赖于一个健康的血管系统。对血管成像的传统标准临床方法是 FA 成像，通过注射荧光素钠使其发射荧光从而提高对比度。FA 和 AOSLO 的结合囊括了高对比度和高分辨率的优点，以远高于传统荧光成像方法的成像质量实现了视网膜黄斑区域的微血管清晰成像[96]，如图 10(a)所示。尽管 FA 在临床上是一种非常有效的血管成像手段，但其是侵入性的，会对人体造成伤害，且成像所需要的时间较长，因此难以做到广泛应用。

AOSLO 具有高分辨率、可实时动态成像的特性，使其可以对毛细血管内运动的血细胞进行成像[68]。视网膜中的大部分组织的散射特性都保持稳定，而血细胞的运动产生了一个在静态背景下的动态信号，也称运动对比度。AOSLO 不需要任何外源性造影剂，通过处理运动对比度便可以非侵入性地构建视网膜副中央凹的血管灌注图，生成视网膜毛细血管网络的高分辨率图像[64,97-98]，如图 10(b)所示。这种方法的缺点在于视网膜运动伪影会导致血管灌注图出现错误，以及对血液流速较慢的血管成像比较困难[99]。

一些非共焦 AOSLO 探测方法如偏置小孔、暗场、分裂探测等也能实现非侵入性的血管成像。共焦 AOSLO 中隔绝掉的多重散射光穿透了视网膜脉络膜，同时该散射光包含着大量有价值的视网膜结构信息。通过收集多重散射光，非共焦 AOSLO 不仅能够提供与 AOSLO FA 类似的血管灌注图，同时也增加了血管壁的可见性，凸显了血管壁的精细结构，特别是在对小动脉壁成像时的效果十分显著，如图 10(c)、(d)、(e)所示。

借助于 AOSLO 对血管系统的多种高分辨率成像方法和研究微血管的能力，血管系统的各项结构参数得以被精确测量。常见的指标有血管内径和外径、血管壁厚度、壁腔比、血管横截面积以及微血管密度[100-105]等。结构参数的测量有助于进一步研究结构参数和眼底疾病之间的关系，定量评估糖尿病性视网膜病变、高血压眼病、青光眼等疾病的发展进程，推动对眼底疾病更深入地理解和治疗。

4.1.3　其他视网膜结构

视网膜总共包含 10 层不同形态的组织结构，除了光感受器细胞和血管系统这两个最重要的视网膜组织

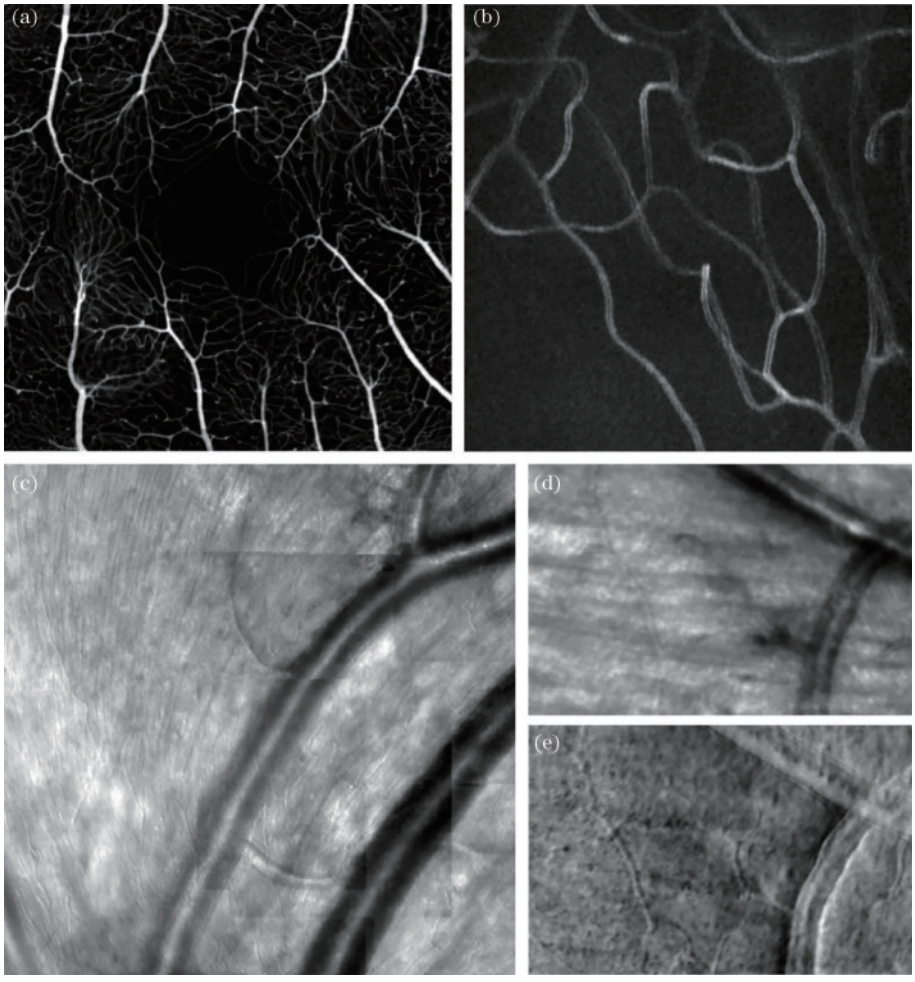

图 10 视网膜血管成像。(a) 中央凹无血管区 AOSLO FA 图[96];(b) 中央凹无血管区运动对比血管灌注图[98];(c) 偏置小孔 AOSLO 获得的视网膜神经乳头凹周围毛细血管图[74];(d) 暗场 AOSLO 获得的中央凹鼻侧 5°偏心处毛细血管图[98];(e) 分裂探测 AOSLO 获得的(d)中同区域毛细血管图[98]

Fig. 10 Retinal vascular imaging. (a) AOSLO FA map of central foveal avascular area[96]; (b) contrast vascular perfusion map of central foveal avascular area movement[98]; (c) capillary diagram around retinal nerve papillary fossa obtained by offset pinhole AOSLO[74]; (d) capillary map at 5° eccentricity on nasal side of fovea obtained by dark field AOSLO[98]; (e) capillary map of same region in (d) obtained by split-detector AOSLO[98]

结构之外,视网膜中的其他组织结构大部分也能够利用 AOSLO 进行成像。视网膜色素上皮(Retinal pigment epithelium, RPE)细胞处于视网膜最外层,其细胞尺寸较大,且反射率较高,但来自光感受器的反射光通常会掩盖 RPE 细胞的反射光,所以在一般情况下 AOSLO 的共焦探测并不能对 RPE 细胞进行成像,而需采用 AOSLO 非共焦暗场探测方法[52]。神经纤维层(Nerve fiber layer, NFL)由第三神经节细胞的轴突组成,是视网膜中比较亮的结构,也是青光眼导致视网膜发生病变的主要区域,通过 AOSLO 可以清晰看见 NFL 的束状结构[106],采用偏振探测成像的方法还可以测量其厚度[107]。与 NFL 类似,黄斑区光感受器细胞的轴突和双极细胞的突起、水平细胞的树突相互连接形成了亨利纤维层,但亨利纤维层的走向倾斜,不与成像光束相互垂直,因此一般情况下不可见,某些眼底病变会导致其走向发生改变,从而使其能够利用 AOSLO 进行成像[108]。神经节细胞(Ganglion cells, GCs)的尺寸相对较大,但其反射率很低,基本无法直接对其成像。目前使用 AOSLO 对 GCs 成像大多数结合了荧光标记技术,而且成像对象仅限于小鼠[109-111]和猕猴[112],尚未应用于人体。筛板(Lamina cribrosa, LC)位于视盘,是层状孔结构,视网膜血管和视神经纤维穿过此结构进出眼球,筛板的形态学改变可能是视神经元损伤的起源,从而导致青光眼的病情。尽管 AOSLO 不能清晰地分辨筛板的立体结构,但其正面图像可以被清晰分辨[113]。与 GCs 类似,双极细胞的尺寸相对较大,但其反射率非常低,同时可能缺少相关的荧光标签,导致其难以被看见,因此目前仍然没有相关的报道称实现了双极细胞的 AOSLO 成像。

4.2 视网膜功能性成像

视网膜结构的高分辨率成像是在细胞尺度评估和治疗视网膜疾病上迈出的关键一步,然而,表面的结构

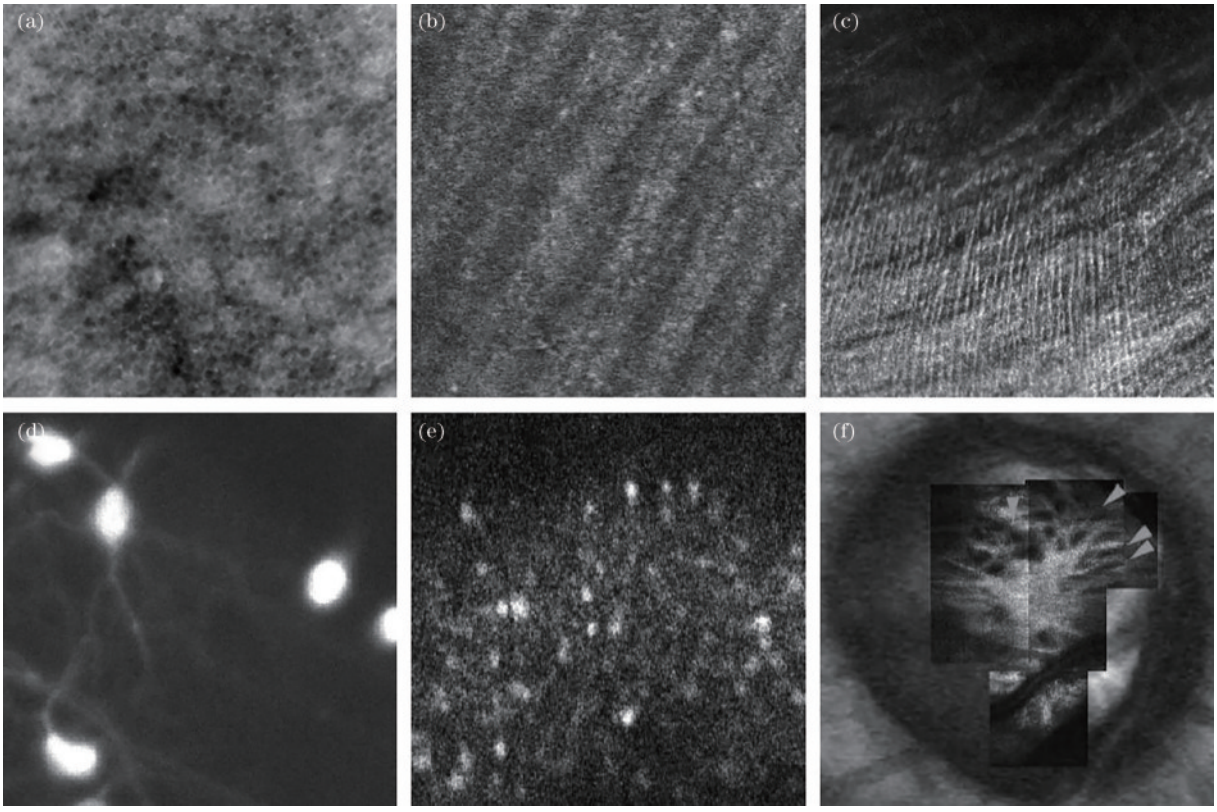

图 11 AOSLO对各类视网膜组织结构的成像结果。(a)健康人眼的RPE图[52];(b)倾斜束状结构为颞侧的NFL[106];(c)垂直细束状结构为亨利纤维,背景较大的横向倾斜束状结构为NFL[108];(d)小鼠GCs的G-CaMP3标记荧光图像[111];(e)猕猴GCs的G-CaMP5标记荧光图像[112];(f)海德堡开发的HRA SLO获取的视盘图像,其上叠加了AOSLO获取的LC图像,箭头处可看见清晰的LC结构[113]

Fig. 11 AOSLO imaging results of various retinal tissue structures. (a) RPE image of healthy human eyes[52]; (b) tilted bundle structure is temporal NFL[106]; (c) vertical fine bundle structure is Henry fibers, while larger transverse inclined bundle structure with larger background is NFL[108]; (d) G-CaMP3 labeled fluorescence images of mouse GCs[111]; (e) G-CaMP5 labeled fluorescence images of GCs in macaques[112]; (f) HRA SLO video disc image developed by Heidelberg is overlaid with LC image obtained by AOSLO, and clear LC structure can be seen at arrow[113]

并不能完整地反映出视网膜的功能信息,若要评估更加完整准确,还需进一步理解视网膜结构表层之下所蕴藏的功能信息。

借助AOSLO分辨单个视锥细胞以及将光束引导到靶向细胞上的能力,彩色视觉的研究能够在单个视锥细胞尺度上进行。研究发现[114],相同类型的视锥细胞能够产生不同的视觉感知,当刺激单一的视锥细胞时,仅有小部分能产生彩色视觉感知,而大部分无法分辨颜色,因此单个视锥细胞和整体的彩色视觉感知之间的联系仍然需要深入研究。当在AOSLO中使用相干光成像时,光感受器反射率会随时空变化,其来源对诊疗有巨大的潜在作用[115]。使用长相干光成像时,研究发现视锥细胞的反射率变化与其方向变化无关,这可能与外节段的长度变化以及内外节段交界处圆盘的产生和脱落有关[116]。而当使用部分相干光时,引起光感受器反射率变化的来源尚不明确[117-118]。光感受器反射率与功能之间的联系尚未被完全发现,基于AOSLO研究视觉产生机制的工作仍在继续[119-122]。

AOSLO具备对视网膜血管的血流进行高速率成像的能力,使其能够跟踪血细胞,不仅可以用于生成微血管的运动对比度灌注图,还可以定量分析微血管内的血流速度,并据此精确地计算出血流量[123]。微血管的功能特性可以根据血流量来评估。利用AOSLO观察到局部性的光刺激引起了局部视网膜小动脉的血流量增加,从而导致了功能性充血,这种现象证明了局部性神经激活会导致血流再分布的观点,也直接证明了功能性充血是受神经血管耦合机制介导的[124-125]。

对视网膜血氧饱和度的测量需要使用不同波长的光,但由于不同波长光的图像差异以及血管的轮廓难以检测,传统的检眼镜即使能对直径50 μm以下的小血管成像,也很难对其进行血氧饱和度测量[126-127]。中国科学院光电所李昊等人利用AOSLO对不同波长光进行像差补偿,使不同波长的图像达到衍射极限分辨率,实现了直径50 μm以下的视网膜毛细血管血氧饱和度的无创测量,结果表明动脉血氧饱和度要明显高于静脉血氧饱和度[45]。视网膜缺氧被认为是引起糖尿病性视网膜病变、视网膜静脉阻塞、青光眼等视网膜疾病的重要因素[128-130],而毛细血管血氧饱和度的测量有

利于诊断此类疾病，并监测其发展进程。

5 挑战与未来发展

CSLO技术经过不断地发展和改进，在超广角眼底成像和高分辨率眼底成像的应用上取得了诸多突破，但时至今日，CSLO在临床应用上仍面临着诸多挑战。

超广角成像的CSLO已经大规模应用于临床，但是在成像视场上仍有局限性，即便是目前成像视场最大的英国欧堡医疗集团的Optos，单次成像具备200°的视场，也只能覆盖大约80%的视网膜面积，仍然无法一次性覆盖到整个视网膜。尽管英国欧堡医疗集团的Optos能通过眼位引导和自动图像拼接技术将眼底检查范围扩大至220°，覆盖约97%的视网膜面积，但仍有可能漏诊如锯齿缘截离裂孔这种位于视网膜锯齿缘的眼底疾病。因此，超广角眼底成像技术可实现全视网膜成像的最终目标，有助于眼底信息的完整呈现，以及视网膜周边眼底疾病识别准确率的提高。而当立体弯曲的视网膜投影到二维平面进行成像时会导致图像周边出现失真和分辨率降低，如果没有对图像进行标定，图像上的距离和面积可能与实际值不一致。未来随着立体投影等算法的引入，这个问题将会得以解决或改善。此外，超广角CSLO的大焦深会使视网膜前方结构包括睫毛、眼睑、玻璃体混浊等在视网膜图像中造成伪影，影响图像质量和诊断结果可利用额外工具如开睑器，或者图像处理方法来减少这些问题给图像质量带来的影响。目前，尚且缺少用于各类视网膜疾病自动检测和分级的图像分析软件，开发配套的图像分析软件，进一步完善超广角CSLO的诊疗流程，将有助于提高视网膜周边病变的识别准确率和效率，以及疾病的治愈率。最后，商用超广角CSLO的成像帧率低的问题也限制了其应用范围的扩大，这个问题将会随着线扫描、多光束扫描等新型成像扫描方式的引入，以及更高速的扫描振镜的出现而得到改善。

超广角CSLO的未来发展，不仅仅要解决技术上现有的问题，也同样应该注重在技术上的应用。例如，利用超广角CSLO获得的眼底图像推动电子病历逐渐替代纸质病历，或是研究其在远程医疗中的应用，都会进一步细化和优化超广角CSLO的应用。

在单细胞高分辨率成像AOSLO方面，该技术在科学研究中取得了非常丰硕的成果，但是从实验室走向真正的临床应用，仍面临不少阻碍。在应用上，其中最大的阻碍之一可能是缺乏一个标准的可供参考的临床应用程序，这也是目前基本没有相关设备获得监管机构批准应用于临床的原因之一。在技术上，现有的AOSLO系统仍存在不少缺陷，例如：1）成像视场仍然太小，难以在不同的时间对同一个区域成像；2）患者的状况包括玻璃体混浊、干眼症、注视震颤等因素容易导致AO闭环失效，从而导致图像质量下降；3）目前缺乏配套的快速图像处理和分析的工具；4）在使用快速扫描振镜成像时可能会引起扫描失真和引入额外的像差[131]。此外，对于临床人员来说，他们缺乏设备操作培训和设备维护的知识，而高昂的设备成本和较大的设备尺寸也使大部分机构难以承受。

为了使AOSLO尽早进入临床应用，首先需要确定AOSLO在临床应用中的准确性和可重复性，确定常规临床应用的有效性和适用范围，得出一个标准化的临床应用程序。其次，将设备集成化和小型化[132]，同时简化操作流程，进一步结合无波前传感AO技术[133]和计算AO技术[134]以降低设备成本。解决成像视场太小的问题将成为未来发展的决定性方向，可以利用扩大AOSLO的成像视场的方法来解决该问题。目前，多层共轭自适应光学技术[88,135]和快速图像拼接技术[136-137]，以及多光瞳成像技术[138]等，均致力于提高单细胞成像视场的分辨率。此外，还应该开发更准确、更快速的图像处理与分析软件[139]，并进一步克服由瞳孔衍射引起的波前像差，实现超高分辨率成像[140-141]。尽管AOSLO存在不少的局限，但单细胞高分辨率成像技术无疑是未来不可避免的趋势，一旦解决这些局限，将会建立起全新的单细胞高分辨率诊疗标准，实现眼底疾病的早期诊断与治疗。

临床应用的要求对眼底疾病的理解应该做到详尽准确，然而，任何单一的成像模式，其成像能力都是有限的，即便是CSLO也无法获取所有的眼底结构信息，多模态CSLO的出现弥补了这一缺陷[142]，使多角度研究眼底疾病成为可能[143-145]。与另一种眼底成像方式光学相干层析（Optical coherence tomography，OCT）相比，CSLO能在正面的眼底图像质量上获得绝对优势，但其纵向成像的能力却落后于OCT[146]。对于纵向分布的眼底结构如内网状层、亨利纤维层等，OCT的成像效果明显优于CSLO[147-149]。此外，对于眼底中因反射率低而无法被CSLO成像的透明结构如GCs、双极细胞等，OCT也能作为补充对这些结构进行成像[150-151]。因此，为了使获得的眼底结构信息尽可能全面，多模态CSLO的发展是十分有必要的。到目前为止，CSLO已经实现了OCT[152-153]、逆行成像[154-155]、分裂探测[51,156]、光声成像[157-158]、荧光成像[159]、多色成像[160-161]等成像模态的整合，并成功应用于人眼眼底成像。双光子CSLO由于需要使用瞬时功率非常高的飞秒激光，因此长期以来都只能应用于动物实验[162-163]。目前，有研究者通过控制激发光的时间特性提高双光子激发效率[164]，结合定制的低功率光纤激光器和智能数据后处理程序，在2022年成功对人眼视网膜进行双光子成像[165]。在未来，CSLO应该扩展更多的成像模态，推动谐波成像[166]、多光子成像[167]等技术在人眼中的应用，形成各个成像模态之间的优势互补，多方面揭示眼底结构的信息，从而增加对眼底疾病的理解。

近年来，人工智能的蓬勃发展极大助力了生物医

学光子学的发展[168]，也同样给CSLO带来了新的发展契机。可以预见的是，人工智能在CSLO中的应用，会主要集中在：1）加速光学设计的优化，缩短系统的开发时间[169-171]；2）优化AO的控制回路，提高AO的校正速度和校正精度[172-176]；3）简化图像后处理流程，减少人工投入并进一步提高图像质量[177-180]；4）提高图像分析速度，得出更为准确可靠的图像解释[181-187]。人工智能与CSLO的结合，势必会进一步发掘CSLO的潜力，提高眼底疾病的筛查率和治愈率，推动CSLO的推广普及。

6 结束语

共聚焦激光扫描检眼镜在过去四十多年得到了显著的发展，不仅推动人眼眼底成像相关的研究向更大成像视场和更精细成像分辨率的方向发展，还为人们提供了对各类眼底疾病新的认识，同时还揭示了许多新的科学发现。随着技术的不断发展，共聚焦激光扫描检眼镜将会更加深入地应用于临床应用和科学研究，揭示各类眼底疾病的发病机制以及视觉产生与视网膜结构之间的联系，提高患者治疗的准确性和有效性。

参 考 文 献

[1] 李凤鸣，谢立信. 中华眼科学[M]. 3版. 北京：人民卫生出版社，2014.
Li F M, Xie L X. Chinese ophthalmology[M]. 3rd ed. Beijing: People's Medical Publishing House, 2014.

[2] Vilela M, Mengue C. Central serous chorioretinopathy classification[J]. Pharmaceuticals, 2020, 14(1): 26.

[3] Pierru A, Girmens J F, Héron E, et al. Occlusions veineuses rétiniennes[J]. Journal Français D'Ophtalmologie, 2017, 40(8): 696-705.

[4] Hendrick A M, Gibson M V, Kulshreshtha A. Diabetic retinopathy[J]. Primary Care: Clinics in Office Practice, 2015, 42(3): 451-464.

[5] Mehta S. Age-related macular degeneration[J]. Primary Care, 2015, 42(3): 377-391.

[6] Ozawa G. Fundus fluorescein and indocyanine green angiography: a textbook and atlas[J]. Optometry and Vision Science, 2009, 86(2): 1018.

[7] Webb R H, Hughes G W, Pomerantzeff O. Flying spot TV ophthalmoscope[J]. Applied Optics, 1980, 19(17): 2991-2997.

[8] Webb R H, Hughes G W, Delori F C. Confocal scanning laser ophthalmoscope[J]. Applied Optics, 1987, 26(8): 1492-1499.

[9] Roorda A, Duncan J L. Adaptive optics ophthalmoscopy [J]. Annual Review of Vision Science, 2015, 1: 19-50.

[10] Choudhry N, Duker J S, Freund K B, et al. Classification and guidelines for widefield imaging: recommendations from the international widefield imaging study group[J]. Ophthalmology: Retina, 2019, 3(10): 843-849.

[11] Pomerantzeff O, Govignon J. Design of a wide-angle ophthalmoscope[J]. Archives of Ophthalmology, 1971, 86(4): 420-424.

[12] Pomerantzeff O. Equator-plus camera[J]. Investigative Ophthalmology, 1975, 14(5): 401-406.

[13] Nakagawa T A, Skrinska R. Improved documentation of retinal hemorrhages using a wide-field digital ophthalmic camera in patients who experienced abusive head trauma [J]. Archives of Pediatrics & Adolescent Medicine, 2001, 155(10): 1149-1152.

[14] Shields C L, Materin M, Shields J A. Panoramic imaging of the ocular fundus[J]. Archives of Ophthalmology, 2003, 121(11): 1603-1607.

[15] Mainster M A, Timberlake G T, Webb R H, et al. Scanning laser ophthalmoscopy[J]. Ophthalmology, 1982, 89(7): 852-857.

[16] Staurenghi G, Viola F, Mainster M A, et al. Scanning laser ophthalmoscopy and angiography with a wide-field contact lens system[J]. Archives of Ophthalmology, 2005, 123(2): 244-252.

[17] Ozerdem U, Freeman W R, Bartsch D U, et al. A simple noncontact wide-angle fundus photography procedure for clinical and research use[J]. Retina, 2001, 21(2): 189-190.

[18] Pomerantzeff O. Wide-angle noncontact and small-angle contact cameras[J]. Investigative Ophthalmology & Visual Science, 1980, 19(8): 973-979.

[19] Friberg T R, Pandya A, Eller A W. Non-mydriatic panoramic fundus imaging using a non-contact scanning laser-based system[J]. Ophthalmic Surgery, Lasers & Imaging, 2003, 34(6): 488-497.

[20] Chalam K V, Brar V S, Keshavamurthy R. Evaluation of modified portable digital camera for screening of diabetic retinopathy[J]. Ophthalmic Research, 2009, 42 (1): 60-62.

[21] Nagiel A, Lalane R A, Sadda S R, et al. Ultra-widefield fundus imaging: a review of clinical applications and future trends[J]. Retina, 2016, 36(4): 660-678.

[22] Ohno-Matsui K. Proposed classification of posterior staphylomas based on analyses of eye shape by three-dimensional magnetic resonance imaging and wide-field fundus imaging[J]. Ophthalmology, 2014, 121(9): 1798-1809.

[23] Croft D E, van Hemert J, Wykoff C C, et al. Precise montaging and metric quantification of retinal surface area from ultra-widefield fundus photography and fluorescein angiography[J]. Ophthalmic Surgery, Lasers & Imaging Retina, 2014, 45(4): 312-317.

[24] Oishi A, Hidaka J, Yoshimura N. Quantification of the image obtained with a wide-field scanning ophthalmoscope [J]. Investigative Ophthalmology & Visual Science, 2014, 55(4): 2424-2431.

[25] Inoue M, Yanagawa A, Yamane S, et al. Wide-field fundus imaging using the Optos Optomap and a disposable eyelid speculum[J]. JAMA Ophthalmology, 2013, 131(2): 226.

[26] Lim W S, Grimaldi G, Nicholson L, et al. Widefield

imaging with Clarus fundus camera vs slit lamp fundus examination in assessing patients referred from the National Health Service diabetic retinopathy screening programme[J]. Eye, 2021, 35(1): 299-306.

[27] Min S G, van Hemert J, Olmos de Koo L C, et al. Assessment of accuracy and precision of quantification of ultra-widefield images[J]. Ophthalmology, 2015, 122(4): 864-866.

[28] Kato Y, Inoue M, Hirakata A. Quantitative comparisons of ultra-widefield images of model eye obtained with Optos® 200Tx and Optos® California[J]. BMC Ophthalmology, 2019, 19(1): 115.

[29] 孔文, 高峰, 樊金宇, 等. 线扫描共聚焦成像技术在生物医学成像中的应用[J]. 激光与光电子学进展, 2018, 55(5): 050003.
Kong W, Gao F, Fan J Y, et al. Application of confocal line scanning imaging technique in biomedical imaging[J]. Laser & Optoelectronics Progress, 2018, 55(5): 050003.

[30] Hammer D X, Ferguson R D, Ustun T E, et al. Line-scanning laser ophthalmoscope[J]. Journal of Biomedical Optics, 2006, 11(4): 041126.

[31] He Y, Li H, Lu J, et al. Retina imaging by using compact line scanning quasi-confocal ophthalmoscope[J]. Chinese Optics Letters, 2013, 11(2): 021101.

[32] Vienola K V, Damodaran M, Braaf B, et al. Parallel line scanning ophthalmoscope for retinal imaging[J]. Optics Letters, 2015, 40(22): 5335-5338.

[33] 刘星宇, 肖昀, 季林, 等. 激光线扫描超广角共聚焦眼底成像[J]. 中国激光, 2023, 50(21): 2107108.
Liu X Y, Xiao Y, Ji L, et al. Ultrawide-angle confocal laser line scanning fundus imaging[J]. Chinese Journal of Lasers, 2023, 50(21): 2107108.

[34] Platisa J, Ye X, Ahrens A M, et al. High-speed low-light in vivo two-photon voltage imaging of large neuronal populations[J]. Nature Methods, 2023, 20(7): 1095-1103.

[35] Choi S, Kim P, Boutilier R, et al. Development of a high speed laser scanning confocal microscope with an acquisition rate up to 200 frames per second[J]. Optics Express, 2013, 21(20): 23611-23618.

[36] Guirao A, Porter J, Williams D R, et al. Calculated impact of higher-order monochromatic aberrations on retinal image quality in a population of human eyes[J]. Journal of the Optical Society of America A, 2002, 19(3): 620-628.

[37] Williams D, Yoon G Y, Porter J, et al. Visual benefit of correcting higher order aberrations of the eye[J]. Journal of Refractive Surgery, 2000, 16(5): S554-S559.

[38] Liu L X, Wu Z Q, Qi M J, et al. Application of adaptive optics in ophthalmology[J]. Photonics, 2022, 9(5): 288.

[39] Lombardo M, Lombardo G. Wave aberration of human eyes and new descriptors of image optical quality and visual performance[J]. Journal of Cataract & Refractive Surgery, 2010, 36(2): 313-331.

[40] Liang J, Williams D R, Miller D T. Supernormal vision and high-resolution retinal imaging through adaptive optics[J]. Journal of the Optical Society of America A, 1997, 14(11): 2884-2892.

[41] Roorda A, Romero-Borja F, Donnelly Iii W, et al. Adaptive optics scanning laser ophthalmoscopy[J]. Optics Express, 2002, 10(9): 405-412.

[42] Ling N, Zhang Y D, Rao X J, et al. Small table-top adaptive optical systems for human retinal imaging[J]. Proceedings of SPIE, 2002, 4825: 99-108.

[43] Ling N, Zhang Y, Rao X, et al. Adaptive optical system for retina imaging approaches clinic applications[M]// Wittrock U. Adaptive optics for industry and medicine. Springer proceedings in physics. Heidelberg: Springer-Verlag, 2006, 102: 305-315.

[44] Shi G H, Dai Y, Wang L, et al. Adaptive optics optical coherence tomography for retina imaging[J]. Chinese Optics Letters, 2008, 6(6): 424-425.

[45] Li H, Lu J, Shi G H, et al. Measurement of oxygen saturation in small retinal vessels with adaptive optics confocal scanning laser ophthalmoscope[J]. Journal of Biomedical Optics, 2011, 16(11): 110504.

[46] Lu J, Li H, Wei L, et al. Retina imaging in vivo with the adaptive optics confocal scanning laser ophthalmoscope [J]. Proceedings of SPIE, 2009, 7519: 75191I.

[47] 卢婧, 李昊, 何毅, 等. 超分辨率活体人眼视网膜共焦扫描成像系统[J]. 物理学报, 2011, 60(3): 034207.
Lu J, Li H, He Y, et al. Superresolution in adaptive optics confocal scanning laser ophthalmoscope[J]. Acta Physica Sinica, 2011, 60(3): 034207.

[48] Burns S A, Elsner A E, Sapoznik K A, et al. Adaptive optics imaging of the human retina[J]. Progress in Retinal and Eye Research, 2019, 68: 1-30.

[49] Cheng T, Liu W J, Pang B Q, et al. A slope-based decoupling algorithm to simultaneously control dual deformable mirrors in a woofer-tweeter adaptive optics system[J]. Chinese Physics B, 2018, 27(7): 070704.

[50] Sulai Y N, Dubra A. Adaptive optics scanning ophthalmoscopy with annular pupils[J]. Biomedical Optics Express, 2012, 3(7): 1647-1661.

[51] Scoles D, Sulai Y N, Langlo C S, et al. In vivo imaging of human cone photoreceptor inner segments[J]. Investigative Ophthalmology & Visual Science, 2014, 55(7): 4244-4251.

[52] Scoles D, Sulai Y N, Dubra A. In vivo dark-field imaging of the retinal pigment epithelium cell mosaic[J]. Biomedical Optics Express, 2013, 4(9): 1710-1723.

[53] Yang Q, Zhang J, Nozato K, et al. Closed-loop optical stabilization and digital image registration in adaptive optics scanning light ophthalmoscopy[J]. Biomedical Optics Express, 2014, 5(9): 3174-3191.

[54] Dubra A, Harvey Z. Registration of 2D images from fast scanning ophthalmic instruments[M]//Fischer B, Dawant B M, Lorenz C. Biomedical image registration. Lecture notes in computer science. Heidelberg: Springer, 2010, 6204: 60-71.

[55] Dubra A, Sulai Y. Reflective afocal broadband adaptive optics scanning ophthalmoscope[J]. Biomedical Optics Express, 2011, 2(6): 1757-1768.

[56] Dubra A, Sulai Y, Norris J L, et al. Noninvasive

imaging of the human rod photoreceptor mosaic using a confocal adaptive optics scanning ophthalmoscope[J]. Biomedical Optics Express, 2011, 2(7): 1864-1876.

[57] Rossi E A, Granger C E, Sharma R, et al. Imaging individual neurons in the retinal ganglion cell layer of the living eye[J]. Proceedings of the National Academy of Sciences of the United States of America, 2017, 114(3): 586-591.

[58] Zhang Y H, Poonja S, Roorda A. MEMS-based adaptive optics scanning laser ophthalmoscopy[J]. Optics Letters, 2006, 31(9): 1268-1270.

[59] Poonja S, Patel S, Henry L, et al. Dynamic visual stimulus presentation in an adaptive optics scanning laser ophthalmoscope[J]. Journal of Refractive Surgery, 2005, 21(5): S575-S580.

[60] Arathorn D W, Yang Q, Vogel C R, et al. Retinally stabilized cone-targeted stimulus delivery[J]. Optics Express, 2007, 15(21): 13731-13744.

[61] Vogel C R, Arathorn D W, Roorda A, et al. Retinal motion estimation in adaptive optics scanning laser ophthalmoscopy[J]. Optics Express, 2006, 14(2): 487-497.

[62] Tuten W S, Tiruveedhula P, Roorda A. Adaptive optics scanning laser ophthalmoscope-based microperimetry[J]. Optometry and Vision Science, 2012, 89(5): 563-574.

[63] Sheehy C K, Tiruveedhula P, Sabesan R, et al. Active eye-tracking for an adaptive optics scanning laser ophthalmoscope[J]. Biomedical Optics Express, 2015, 6(7): 2412-2423.

[64] Tam J, Martin J A, Roorda A. Noninvasive visualization and analysis of parafoveal capillaries in humans[J]. Investigative Ophthalmology & Visual Science, 2010, 51(3): 1691-1698.

[65] Mozaffari S, Jaedicke V, LaRocca F, et al. Versatile multi-detector scheme for adaptive optics scanning laser ophthalmoscopy[J]. Biomedical Optics Express, 2018, 9(11): 5477-5488.

[66] Grieve K, Tiruveedhula P, Zhang Y H, et al. Multi-wavelength imaging with the adaptive optics scanning laser Ophthalmoscope[J]. Optics Express, 2006, 14(25): 12230-12242.

[67] Mozaffari S, LaRocca F, Jaedicke V, et al. Wide-vergence, multi-spectral adaptive optics scanning laser ophthalmoscope with diffraction-limited illumination and collection[J]. Biomedical Optics Express, 2020, 11(3): 1617-1632.

[68] Martin J A, Roorda A. Direct and noninvasive assessment of parafoveal capillary leukocyte velocity[J]. Ophthalmology, 2005, 112(12): 2219-2224.

[69] Bowers N R, Boehm A E, Roorda A. The effects of fixational tremor on the retinal image[J]. Journal of Vision, 2019, 19(11): 8.

[70] Bowers N R, Gautier J, Lin S, et al. Fixational eye movements in passive versus active sustained fixation tasks[J]. Journal of Vision, 2021, 21(11): 16.

[71] Hammer D X, Ferguson R D, Bigelow C E, et al. Adaptive optics scanning laser ophthalmoscope for stabilized retinal imaging[J]. Optics Express, 2006, 14(8): 3354-3367.

[72] Burns S A, Tumbar R, Elsner A E, et al. Large-field-of-view, modular, stabilized, adaptive-optics-based scanning laser ophthalmoscope[J]. Journal of the Optical Society of America A, 2007, 24(5): 1313-1326.

[73] Ferguson R D, Zhong Z Y, Hammer D X, et al. Adaptive optics scanning laser ophthalmoscope with integrated wide-field retinal imaging and tracking[J]. Journal of the Optical Society of America A, 2010, 27(11): A265-A277.

[74] Chui T Y P, Vannasdale D A, Burns S A. The use of forward scatter to improve retinal vascular imaging with an adaptive optics scanning laser ophthalmoscope[J]. Biomedical Optics Express, 2012, 3(10): 2537-2549.

[75] Chui T Y P, Gast T J, Burns S A. Imaging of vascular wall fine structure in the human retina using adaptive optics scanning laser ophthalmoscopy[J]. Investigative Ophthalmology & Visual Science, 2013, 54(10): 7115-7124.

[76] Zhong Z Y, Petrig B L, Qi X F, et al. In vivo measurement of erythrocyte velocity and retinal blood flow using adaptive optics scanning laser ophthalmoscopy [J]. Optics Express, 2008, 16(17): 12746-12756.

[77] Zhong Z Y, Song H X, Chui T Y P, et al. Noninvasive measurements and analysis of blood velocity profiles in human retinal vessels[J]. Investigative Ophthalmology & Visual Science, 2011, 52(7): 4151-4157.

[78] Song H X, Zhao Y M, Qi X F, et al. Stokes vector analysis of adaptive optics images of the retina[J]. Optics Letters, 2008, 33(2): 137-139.

[79] Song H X, Qi X F, Zou W Y, et al. Dual electro-optical modulator polarimeter based on adaptive optics scanning laser ophthalmoscope[J]. Optics Express, 2010, 18(21): 21892-21904.

[80] de Castro A, Huang G, Sawides L, et al. Rapid high resolution imaging with a dual-channel scanning technique [J]. Optics Letters, 2016, 41(8): 1881-1884.

[81] Mujat M, Ferguson R D, Iftimia N, et al. Compact adaptive optics line scanning ophthalmoscope[J]. Optics Express, 2009, 17(12): 10242-10258.

[82] Luo T, Warner R L, Sapoznik K A, et al. Template free eye motion correction for scanning systems[J]. Optics Letters, 2021, 46(4): 753-756.

[83] Li H, Yang H S, Shi G H, et al. Adaptive optics retinal image registration from scale-invariant feature transform [J]. Optik, 2011, 122(9): 839-841.

[84] Li H, Lu J, Shi G H, et al. Tracking features in retinal images of adaptive optics confocal scanning laser ophthalmoscope using KLT-SIFT algorithm[J]. Biomedical Optics Express, 2010, 1(1): 31-40.

[85] Li H, Lu J, Shi G H, et al. Automatic montage of retinal images in adaptive optics confocal scanning laser ophthalmoscope[J]. Optical Engineering, 2012, 51(5): 057008.

[86] He Y, Deng G H, Wei L, et al. Design of a compact, bimorph deformable mirror-based adaptive optics scanning

laser ophthalmoscope[M]//Luo Q M, Li L Z, Harrison D K, et al. Oxygen transport to tissue XXXVIII. Advances in experimental medicine and biology. Cham: Springer, 2016, 923: 375-383.

[87] Wang Y Y, He Y, Wei L, et al. Bimorph deformable mirror based adaptive optics scanning laser ophthalmoscope for retina imaging in vivo[J]. Chinese Optics Letters, 2017, 15(12): 121102.

[88] Laslandes M, Salas M, Hitzenberger C K, et al. Increasing the field of view of adaptive optics scanning laser ophthalmoscopy[J]. Biomedical Optics Express, 2017, 8(11): 4811-4826.

[89] Roorda A, Williams D R. Optical fiber properties of individual human cones[J]. Journal of Vision, 2002, 2(5): 404-412.

[90] Meadway A, Sincich L C. Light reflectivity and interference in cone photoreceptors[J]. Biomedical Optics Express, 2019, 10(12): 6531-6554.

[91] Chiu S J, Lokhnygina Y, Dubis A M, et al. Automatic cone photoreceptor segmentation using graph theory and dynamic programming[J]. Biomedical Optics Express, 2013, 4(6): 924-937.

[92] Chen Y W, He Y, Wang J, et al. Automated superpixels-based identification and mosaicking of cone photoreceptor cells for adaptive optics scanning laser ophthalmoscope[J]. Chinese Optics Letters, 2020, 18(10): 101701.

[93] Cooper R F, Wilk M A, Tarima S, et al. Evaluating descriptive metrics of the human cone mosaic[J]. Investigative Ophthalmology & Visual Science, 2016, 57(7): 2992-3001.

[94] Wells-Gray E M, Choi S S, Bries A, et al. Variation in rod and cone density from the fovea to the mid-periphery in healthy human retinas using adaptive optics scanning laser ophthalmoscopy[J]. Eye, 2016, 30(8): 1135-1143.

[95] Sawides L, de Castro A, Burns S A. The organization of the cone photoreceptor mosaic measured in the living human retina[J]. Vision Research, 2017, 132: 34-44.

[96] Pinhas A, Dubow M, Shah N, et al. In vivo imaging of human retinal microvasculature using adaptive optics scanning light ophthalmoscope fluorescein angiography [J]. Biomedical Optics Express, 2013, 4(8): 1305-1317.

[97] Gu B Y, Wang X L, Twa M D, et al. Noninvasive in vivo characterization of erythrocyte motion in human retinal capillaries using high-speed adaptive optics near-confocal imaging[J]. Biomedical Optics Express, 2018, 9(8): 3653-3677.

[98] Sulai Y N, Scoles D, Harvey Z, et al. Visualization of retinal vascular structure and perfusion with a nonconfocal adaptive optics scanning light ophthalmoscope[J]. Journal of the Optical Society of America A, 2014, 31(3): 569-579.

[99] Chui T Y P, Mo S, Krawitz B, et al. Human retinal microvascular imaging using adaptive optics scanning light ophthalmoscopy[J]. International Journal of Retina and Vitreous, 2016, 2: 11.

[100] Hillard J G, Gast T J, Chui T Y P, et al. Retinal arterioles in hypo-, normo-, and hypertensive subjects measured using adaptive optics[J]. Translational Vision Science & Technology, 2016, 5(4): 16.

[101] Arichika S, Uji A, Murakami T, et al. Correlation of retinal arterial wall thickness with atherosclerosis predictors in type 2 diabetes without clinical retinopathy [J]. The British Journal of Ophthalmology, 2017, 101(1): 69-74.

[102] Arichika S, Uji A, Ooto S, et al. Effects of age and blood pressure on the retinal arterial wall, analyzed using adaptive optics scanning laser ophthalmoscopy[J]. Scientific Reports, 2015, 5: 12283.

[103] Chui T Y P, Pinhas A, Gan A, et al. Longitudinal imaging of microvascular remodelling in proliferative diabetic retinopathy using adaptive optics scanning light ophthalmoscopy[J]. Ophthalmic & Physiological Optics, 2016, 36(3): 290-302.

[104] Pinhas A, Dubow M, Shah N, et al. Fellow eye changes in patients with nonischemic central retinal vein occlusion: assessment of perfused foveal microvascular density and identification of nonperfused capillaries[J]. Retina, 2015, 35(10): 2028-2036.

[105] Nesper P L, Scarinci F, Fawzi A A. Adaptive optics reveals photoreceptor abnormalities in diabetic macular ischemia[J]. PLoS One, 2017, 12(1): e0169926.

[106] Takayama K, Ooto S, Hangai M, et al. High-resolution imaging of the retinal nerve fiber layer in normal eyes using adaptive optics scanning laser ophthalmoscopy[J]. PLoS One, 2012, 7(3): e33158.

[107] da Pozzo S, Marchesan R, Ravalico G. Scanning laser polarimetry-a review[J]. Clinical & Experimental Ophthalmology, 2009, 37(1): 68-80.

[108] Scoles D, Higgins B P, Cooper R F, et al. Microscopic inner retinal hyper-reflective phenotypes in retinal and neurologic disease[J]. Investigative Ophthalmology & Visual Science, 2014, 55(7): 4015-4029.

[109] Cheong S K, Strazzeri J M, Williams D R, et al. All-optical recording and stimulation of retinal neurons in vivo in retinal degeneration mice[J]. PLoS One, 2018, 13(3): e0194947.

[110] Geng Y, Dubra A, Yin L, et al. Adaptive optics retinal imaging in the living mouse eye[J]. Biomedical Optics Express, 2012, 3(4): 715-734.

[111] Yin L, Geng Y, Osakada F, et al. Imaging light responses of retinal ganglion cells in the living mouse eye [J]. Journal of Neurophysiology, 2013, 109(9): 2415-2421.

[112] Yin L, Masella B, Dalkara D, et al. Imaging light responses of foveal ganglion cells in the living macaque eye[J]. The Journal of Neuroscience, 2014, 34(19): 6596-6605.

[113] Akagi T, Hangai M, Takayama K, et al. In vivo imaging of lamina cribrosa pores by adaptive optics scanning laser ophthalmoscopy[J]. Investigative Ophthalmology & Visual Science, 2012, 53(7): 4111-4119.

[114] Sabesan R, Schmidt B P, Tuten W S, et al. The elementary representation of spatial and color vision in

the human retina[J]. Science Advances, 2016, 2(9): e1600797.

[115] Grieve K, Roorda A. Intrinsic signals from human cone photoreceptors[J]. Investigative Ophthalmology & Visual Science, 2008, 49(2): 713-719.

[116] Pircher M, Kroisamer J S, Felberer F, et al. Temporal changes of human cone photoreceptors observed in vivo with SLO/OCT[J]. Biomedical Optics Express, 2010, 2(1): 100-112.

[117] Cooper R F, Dubis A M, Pavaskar A, et al. Spatial and temporal variation of rod photoreceptor reflectance in the human retina[J]. Biomedical Optics Express, 2011, 2(9): 2577-2589.

[118] Rha J, Schroeder B, Godara P, et al. Variable optical activation of human cone photoreceptors visualized using a short coherence light source[J]. Optics Letters, 2009, 34(24): 3782-3784.

[119] Tuten W S, Harmening W M, Sabesan R, et al. Spatiochromatic interactions between individual cone photoreceptors in the human retina[J]. The Journal of Neuroscience, 2017, 37(39): 9498-9509.

[120] Domdei N, Domdei L, Reiniger J L, et al. Ultra-high contrast retinal display system for single photoreceptor psychophysics[J]. Biomedical Optics Express, 2017, 9(1): 157-172.

[121] Schmidt B P, Boehm A E, Foote K G, et al. The spectral identity of foveal cones is preserved in hue perception[J]. Journal of Vision, 2018, 18(11): 19.

[122] Schmidt B P, Boehm A E, Tuten W S, et al. Spatial summation of individual cones in human color vision[J]. PLoS One, 2019, 14(7): e0211397.

[123] Warner R L, Gast T J, Sapoznik K A, et al. Measuring temporal and spatial variability of red blood cell velocity in human retinal vessels[J]. Investigative Ophthalmology & Visual Science, 2021, 62(14): 29.

[124] Duan A, Bedggood P A, Bui B V, et al. Evidence of flicker-induced functional hyperaemia in the smallest vessels of the human retinal blood supply[J]. PLoS One, 2016, 11(9): e0162621.

[125] Newman E A. Functional hyperemia and mechanisms of neurovascular coupling in the retinal vasculature[J]. Journal of Cerebral Blood Flow and Metabolism, 2013, 33(11): 1685-1695.

[126] Smith M H, Denninghoff K R, Hillman L W, et al. Oxygen saturation measurements of blood in retinal vessels during blood loss[J]. Journal of Biomedical Optics, 1998, 3(3): 296-303.

[127] Delori F C. Noninvasive technique for oximetry of blood in retinal vessels[J]. Applied Optics, 1988, 27(6): 1113-1125.

[128] Yoneya S, Saito T, Nishiyama Y, et al. Retinal oxygen saturation levels in patients with central retinal vein occlusion[3][J]. Ophthalmology, 2002, 109(8): 1521-1526.

[129] Stefansson E, Landers M B, Wolbarsht M L. Oxygenation and vasodilatation in relation to diabetic and other proliferative retinopathies[J]. Ophthalmic Surgery, 1983, 14(3): 209-226.

[130] Arjamaa O, Nikinmaa M. Oxygen-dependent diseases in the retina: role of hypoxia-inducible factors[J]. Experimental Eye Research, 2006, 83(3): 473-483.

[131] Akondi V, Kowalski B, Burns S A, et al. Dynamic distortion in resonant galvanometric optical scanners[J]. Optica, 2020, 7(11): 1506-1513.

[132] DuBose T, Nankivil D, LaRocca F, et al. Handheld adaptive optics scanning laser ophthalmoscope[J]. Optica, 2018, 5(9): 1027-1036.

[133] Hofer H, Sredar N, Queener H, et al. Wavefront sensorless adaptive optics ophthalmoscopy in the human eye[J]. Optics Express, 2011, 19(15): 14160-14171.

[134] Adie S G, Graf B W, Ahmad A, et al. Computational adaptive optics for broadband optical interferometric tomography of biological tissue[J]. Proceedings of the National Academy of Science, 2012, 109(19): 7175-7180.

[135] Furieri T, Bassi A, Bonora S. Large field of view aberrations correction with deformable lenses and multi conjugate adaptive optics[J]. Journal of Biophotonics, 2023, 16(12): e202300104.

[136] Davidson B, Kalitzeos A, Carroll J, et al. Fast adaptive optics scanning light ophthalmoscope retinal montaging [J]. Biomedical Optics Express, 2018, 9(9): 4317-4328.

[137] Chen M, Cooper R F, Gee J C, et al. Automatic longitudinal montaging of adaptive optics retinal images using constellation matching[J]. Biomedical Optics Express, 2019, 10(12): 6476-6496.

[138] Park J H, Kong L J, Zhou Y F, et al. Large-field-of-view imaging by multi-pupil adaptive optics[J]. Nature Methods, 2017, 14(6): 581-583.

[139] Salmon A E, Cooper R F, Chen M, et al. Automated image processing pipeline for adaptive optics scanning light ophthalmoscopy[J]. Biomedical Optics Express, 2021, 12(6): 3142-3168.

[140] Lu R W, Aguilera N, Liu T, et al. In-vivo sub-diffraction adaptive optics imaging of photoreceptors in the human eye with annular pupil illumination and sub-Airy detection[J]. Optica, 2021, 8(3): 333-343.

[141] Lu Y M, Son T, Kim T H, et al. Virtually structured detection enables super-resolution ophthalmoscopy of rod and cone photoreceptors in human retina[J]. Quantitative Imaging in Medicine and Surgery, 2021, 11(3): 1060-1069.

[142] Mujat M, Ferguson R D, Patel A H, et al. High resolution multimodal clinical ophthalmic imaging system [J]. Optics Express, 2010, 18(11): 11607-11621.

[143] Viola F, Barteselli G, Dell'Arti L, et al. Multimodal imaging in deferoxamine retinopathy[J]. Retina, 2014, 34(7): 1428-1438.

[144] Acón D, Wu L. Multimodal imaging in diabetic macular edema[J]. Asia-Pacific Journal of Ophthalmology, 2018, 7(1): 22-27.

[145] Paavo M, Lee W, Parmann R, et al. Insights into PROM1-macular disease using multimodal imaging[J]. Investigative Ophthalmology & Visual Science, 2023, 64(4): 27.

[146] Williams D R, Burns S A, Miller D T, et al. Evolution of adaptive optics retinal imaging[J]. Biomedical Optics Express, 2023, 14(3): 1307-1338.

[147] Kesim C, Bektas S N, Kulali Z, et al. Henle fiber layer mapping with directional optical coherence tomography [J]. Retina, 2022, 42(9): 1780-1787.

[148] Griffin S M, McDonald H R, Johnson R N, et al. Fingerprint sign of the henle fiber layer[J]. Retina, 2021, 41(2): 381-386.

[149] Zhang T W, Kho A M, Srinivasan V J. *In vivo* morphometry of inner plexiform layer (IPL) stratification in the human retina with visible light optical coherence tomography[J]. Frontiers in Cellular Neuroscience, 2021, 15: 655096.

[150] Liu Z L, Kurokawa K, Zhang F R, et al. Imaging and quantifying ganglion cells and other transparent neurons in the living human retina[J]. Proceedings of the National Academy of Sciences of the United States of America, 2017, 114(48): 12803-12808.

[151] Pfäffle C, Spahr H, Gercke K, et al. Phase-sensitive measurements of depth-dependent signal transduction in the inner plexiform layer[J]. Frontiers in Medicine, 2022, 9: 885187.

[152] Bigelow C E, Iftimia N V, Ferguson R D, et al. Compact multimodal adaptive-optics spectral-domain optical coherence tomography instrument for retinal imaging[J]. Journal of the Optical Society of America A, 2007, 24(5): 1327-1336.

[153] Liu Z L, Zhang F R, Zucca K, et al. Ultrahigh-speed multimodal adaptive optics system for microscopic structural and functional imaging of the human retina[J]. Biomedical Optics Express, 2022, 13(11): 5860-5878.

[154] Azzolini C, Di Nicola M, Pozzo Giuffrida F, et al. Retromode scanning laser ophthalmoscopy for choroidal nevi: a preliminary study[J]. Life, 2023, 13(6): 1253.

[155] Mainster M A, Desmettre T, Querques G, et al. Scanning laser ophthalmoscopy retroillumination: applications and illusions[J]. International Journal of Retina and Vitreous, 2022, 8(1): 71.

[156] Sredar N, Razeen M, Kowalski B, et al. Comparison of confocal and non-confocal split-detection cone photoreceptor imaging[J]. Biomedical Optics Express, 2021, 12(2): 737-755.

[157] Song W, Wei Q, Liu T, et al. Integrating photoacoustic ophthalmoscopy with scanning laser ophthalmoscopy, optical coherence tomography, and fluorescein angiography for a multimodal retinal imaging platform[J]. Journal of Biomedical Optics, 2012, 17(6): 061206.

[158] 赵鹏艳, 陈重江. 多模态光声成像技术及其在眼科学中的应用进展[J]. 激光与光电子学进展, 2022, 59(6): 0617014.
Zhao P Y, Chen C J. Progress of multimodal photoacoustic imaging and its application in ophthalmology [J]. Laser & Optoelectronics Progress, 2022, 59(6): 0617014.

[159] Schweitzer D, Haueisen J, Klemm M. Suppression of natural lens fluorescence in fundus autofluorescence measurements: review of hardware solutions[J]. Biomedical Optics Express, 2022, 13(10): 5151-5170.

[160] Terasaki H, Sonoda S, Tomita M, et al. Recent advances and clinical application of color scanning laser ophthalmoscope[J]. Journal of Clinical Medicine, 2021, 10(4): 718.

[161] Gupta K, Agarwal A, Arora A, et al. Multicolor confocal scanning laser ophthalmoscope imaging in posterior uveitis[J]. Retina, 2022, 42(7): 1356-1363.

[162] Jayabalan G S, Wu Y K, Bille J F, et al. In vivo two-photon imaging of retina in rabbits and rats[J]. Experimental Eye Research, 2018, 166: 40-48.

[163] Palczewska G, Stremplewski P, Suh S, et al. Two-photon imaging of the mammalian retina with ultrafast pulsing laser[J]. JCI Insight, 2018, 3(17): e121555.

[164] Palczewska G, Boguslawski J, Stremplewski P, et al. Noninvasive two-photon optical biopsy of retinal fluorophores[J]. Proceedings of the National Academy of Sciences of the United States of America, 2020, 117 (36): 22532-22543.

[165] Boguslawski J, Palczewska G, Tomczewski S, et al. In vivo imaging of the human eye using a 2-photon-excited fluorescence scanning laser ophthalmoscope[J]. The Journal of Clinical Investigation, 2022, 132(2): e154218.

[166] Aghigh A, Bancelin S, Rivard M, et al. Second harmonic generation microscopy: a powerful tool for bio-imaging[J]. Biophysical Reviews, 2023, 15(1): 43-70.

[167] Miller D R, Jarrett J W, Hassan A M, et al. Deep tissue imaging with multiphoton fluorescence microscopy[J]. Current Opinion in Biomedical Engineering, 2017, 4: 32-39.

[168] Hadad B, Froim S, Yosef E, et al. Deep learning in optics: a tutorial[J]. Journal of Optics, 2023, 25(12): 123501.

[169] Côté G, Lalonde J F, Thibault S. Deep learning-enabled framework for automatic lens design starting point generation[J]. Optics Express, 2021, 29(3): 3841-3854.

[170] Li W Z, Jia X D, Hsu Y M, et al. A novel methodology for lens matching in compact lens module assembly[J]. IEEE Transactions on Automation Science and Engineering, 2023, 20(2): 741-750.

[171] Hegde R S. Accelerating optics design optimizations with deep learning[J]. Optical Engineering, 2019, 58(6): 065103.

[172] Guo Y M, Zhong L B, Min L, et al. Adaptive optics based on machine learning: a review[J]. Opto-Electronic Advances, 2022, 5(7): 200082.

[173] Zhang B W, Zhu J Z, Si K, et al. Deep learning assisted zonal adaptive aberration correction[J]. Frontiers in Physics, 2021, 8: 634.

[174] Hu S W, Hu L J, Gong W, et al. Deep learning based wavefront sensor for complex wavefront detection in adaptive optical microscopes[J]. Frontiers of Information Technology & Electronic Engineering, 2021, 22(10): 1277-1288.

[175] Li Y S, Yue D, He Y H. Prediction of wavefront distortion for wavefront sensorless adaptive optics based on deep learning[J]. Applied Optics, 2022, 61(14): 4168-

4176.

[176] Durech E, Newberry W, Franke J, et al. Wavefront sensor-less adaptive optics using deep reinforcement learning[J]. Biomedical Optics Express, 2021, 12(9): 5423-5438.

[177] Wan C, Zhou X T, You Q J, et al. Retinal image enhancement using cycle-constraint adversarial network [J]. Frontiers in Medicine, 2022, 8: 793726.

[178] Abbood S H, Hamed H N A, Rahim M S M, et al. Hybrid retinal image enhancement algorithm for diabetic retinopathy diagnostic using deep learning model[J]. IEEE Access, 2022, 10: 73079-73086.

[179] Kadomoto S, Uji A, Muraoka Y, et al. Enhanced visualization of retinal microvasculature in optical coherence tomography angiography imaging via deep learning[J]. Journal of Clinical Medicine, 2020, 9(5): 1322.

[180] Devi L M, Wahengbam K, Singh A D. Dehazing buried tissues in retinal fundus images using a multiple radiance pre-processing with deep learning based multiple feature-fusion [J]. Optics & Laser Technology, 2021, 138: 106908.

[181] Subha K J, Rajavel R, Paulchamy B. Improved ensemble deep learning based retinal disease detection using image processing[J]. Journal of Intelligent & Fuzzy Systems, 2023, 45(1): 1119-1130.

[182] Gupta I K, Choubey A, Choubey S. Mayfly optimization with deep learning enabled retinal fundus image classification model[J]. Computers and Electrical Engineering, 2022, 102: 108176.

[183] Cherukuri V, Kumar B G V, Bala R, et al. Deep retinal image segmentation with regularization under geometric priors[J]. IEEE Transactions on Image Processing, 2019, 29: 2552-2567.

[184] Boudegga H, Elloumi Y, Akil M, et al. Fast and efficient retinal blood vessel segmentation method based on deep learning network[J]. Computerized Medical Imaging and Graphics, 2021, 90: 101902.

[185] Zhang Q, Sampani K, Xu M J, et al. AOSLO-net: a deep learning-based method for automatic segmentation of retinal microaneurysms from adaptive optics scanning laser ophthalmoscopy images[J]. Translational Vision Science & Technology, 2022, 11(8): 7.

[186] Cunefare D, Huckenpahler A L, Patterson E J, et al. RAC-CNN: multimodal deep learning based automatic detection and classification of rod and cone photoreceptors in adaptive optics scanning light ophthalmoscope images [J]. Biomedical Optics Express, 2019, 10(8): 3815-3832.

[187] Cunefare D, Langlo C S, Patterson E J, et al. Deep learning based detection of cone photoreceptors with multimodal adaptive optics scanning light ophthalmoscope images of Achromatopsia[J]. Biomedical Optics Express, 2018, 9(8): 3740-3756.